6335



USAELRDL Technical Report 2308

# DESIGN AND EVALUATION OF THERMOELECTRIC THERMAL BARRIER FOR MICRO-MODULES

Robert D. FitzGerald

Herbert C. Frankel





September 1962

UNITED STATES ARMY
ELECTRONICS RESEARCH AND DEVELOPMENT LABORATORY
FORT MONMOUTH, N.J.

U. S. ARMY ELECTRONICS RESEARCH AND DEVELOPMENT LABORATORY

FORT MONMOUTH, NEW JERSEY

September 1962

USAELRDL Technical Report 2308 has been prepared urder the supervision of the Director, Electronic Components Department, and is published for the information and guidance of all concerned. Suggestions or criticisms relative to the form, content, purpose, or use of this publication should be referred to the Commanding Officer, U. S. Army Electronics Research and Development Laboratory, Attn: Chief, Modular Assemblies Branch, Electronic Parts and Materials Division, Fort Monmouth, New Jersey.

J. M. KIMBROUGH, JR.
Colonel, Signal Corps
Commanding

OFFICIAL:
HOWARD W. KILLAM
Major, SigC
Adjutant

DISTRIBUTION:
Special

# DESIGN AND EVALUATION OF THERMOELECTRIC THERMAL BARRIER FOR MICRO-MODULES

Robert D. FitzGerald

Herbert C. Frankel

DA TASK NR. 3A99-15-002-03

## ABSTRACT

This report covers internal work on the use of a specific Peltier temperature control device, called a "thermoelectric thermal barrier," to protect heat-sensitive electronic circuit elements from closely associated heat-producing elements in a microelectronic assembly. Test results on a simulated binary divider micro-module indicate the feasibility of the thermoelectric thermal barrier approach.

U. S. ARMY ELECTRONICS RESEARCH AND DEVELOPMENT LABORATORY

FORT MONMOUTH, NEW JERSEY

## CONTENTS



## TABLES

## CONTENTS



## TABLES

CONTENTS (Contd)

FIGURES



APPENDIX

# DESIGN AND EVALUATION OF THERMOELECTRIC THERMAL BARRIER FOR MICRO-MODULES

## INTRODUCTION

### *Purpose*

The thermoelectric thermal barrier investigation reported herein is part of a USAELRDL internal study on thermoelectric heat transfer devices. This study is the initial effort of a research and development program covering designs for specific thermoelectric devices having an overall superiority in size, weight, performance, and reliability to existing devices for (1) regulating temperatures of temperature sensitive electronic parts and subassemblies, and (2) protecting heat limited parts and subassemblies. The objective of the overall study is (1) to obtain basic information on capabilities, limitations, design procedures, and fabrication of such devices by means of a literature search and experimentation with basic junctions; (2) to evaluate commercially available devices; and (3) to design and fabricate experimental "spot" temperature regulating devices compatible in size with, and capable of cooling, typical Army micro-modules.

This report covers preliminary work on this last objective, using a simulated micro-module as the test vehicle.

### *Background*

1. *Heat Problem in Miniature Equipment:* The thermal design of an electronic equipment is a major determinant of its reliability. Unless effective heat removal is provided, specific electronic parts and subassemblies may become too hot, resulting in malfunction and failure. In recent years, the problem of cooling electronic apparatus has been aggravated by the extra burden imposed by miniaturization, hermetic sealing, and the frictional heat and low air densities associated with such high-speed, high-altitude equipment carriers as missiles and satellites.

An example of particular concern is the heat problem associated with certain micro-modular subassemblies (microassemblies), whose germanium active elements must not be operated at junction temperatures above 100°C, thus limiting the maximum temperature at which the microassemblies can be used. Therefore, it is very important to remove the heat generated by resistors and other heat producing parts by the best practical means.

2. *Present Heat Transfer Methods:* At present, heat in electronic equipment is removed by heat transfer systems employing natural methods (conduction, radiation, natural convection, and evaporation) or forced convection, or combinations of these methods. Forced convection (air or liquid) uses additional energy to provide much higher cooling rates than do the natural methods. However, natural cooling is used to a great extent because such factors as (1) size and weight, (2) additional unreliability and maintenance cost, due to wear of moving parts or corrosive action of refrigerant, and (3) complications, due to dense circuit packaging, may prevent use of forced air and circulating liquid systems. (For discussion of conventional cooling methods for small equipment, see "Heat Transfer in Miniaturized Electronic Equipment," prepared by Cornell Aeronautical Laboratory, Inc., under Bureau of Ships Contract NObsr-49228 (March 1952).)

3. *Advantages of Thermoelectric Method:* Based on advances to date, there is a promise that thermoelectric heat transfer systems for large electronic assemblies will eventually be made

to provide the high cooling rates now obtainable by forced methods, yet will have smaller size and weight, greater reliability and lower maintenance cost (because there are no moving parts or corrosive fluids) than are typical of the forced methods. However, temperature regulation of *"spots"* and *small spaces,* particularly where hermetic sealing, encapsulation or dense circuit packaging are concerned, *even now* may be more advantageously accomplished by thermoelectric, rather than mechanical, heat transfer methods. (For examples of applications, see Reference 33.) Other advantages besides those mentioned or implied above are versatility (i.e., device can be used as a heater which is more efficient than Joule heating by reversing current direction), lack of vibration and noise, and controllable cooling rate to meet existing conditions. For outer space applications, the use of thermoelectric cooling can eliminate the problems of lubrication and coolant circulation encountered in a high vacuum, gravitationless environment.

## APPROACH

Simulated micro-modules with and without built-in thermoelectric temperature regulating devices were constructed and evaluated to demonstrate protection of a heat-sensitive circuit element (e.g., a transistor) against heat produced by heat-generating circuit elements (e.g., resistors) within the same micro-module. This approach was suggested by a problem reported by RCA in the Fifth Quarterly Report on the Army Micro-Module Production Program conducted under Signal Corps Contract No. DA36-039 sc-75968. Construction details and their relation to this problem are discussed in the following "Experimental Apparatus" section.

The temperature regulating device, called a "thermoelectric thermal barrier"* or TETB, consists of a single Peltier couple located between the heat-sensitive and heat-generating elements, with the cold end facing the former. The TETB absorbs net heat from the heat-sensitive element zone and transfers it "electrically" to the heat-generating element zone in a manner discussed later in the "Appendix." As a result, the heat-sensitive elements can be cooled to tolerable temperatures.

This transfer of heat "uphill" from a *colder* to a *warmer* zone is the so-called "refrigeration" mode of operation. Heat transfer from a *warmer* to a *colder* zone is sometimes called "heat pumping" in the literature. Investigators report that the Peltier effect alone is generally not as efficient as a copper rod for such "heat pumping." [26,48]

## EXPERIMENTAL APPARATUS

### *Simulated Micro-Modules*

Several simulated micro-modules were fabricated, including some units for preliminary tests and the two units designated SMM#1 and SMM#2 used in the reported effort.

A diagram of SMM#2, a simulated micro-module with a TETB (described in detail below), is shown in Fig. 1. A heat-sensitive element near the top is simulated by the temperature-measuring thermocouple itself. The resistors simulate a heat-generating element near the bottom.

SMM#1 is similar, except for the omission of the TETB. It was used for comparative measurements.

*Based on device described in Patent Disclosure by R. D. FitzGerald and R. A. Gerhold, Docket No. 12,158 (U. S. Army Electronics Patent Activity), "Thermal Barrier for Micro-Module."

The simulated units are encapsulated in black epoxy. Each simulated unit is 0.40" wide by 0.40" deep by 0.50" high (excluding leads). A typical micro-module is 0.35" wide by 0.35" deep by about 0.4" to 0.5" high (excluding leads). (The slight increase in cross-sectional dimensions resulted from use of an oversize mold, which was the only kind available when the simulated units were made.)

Aside from the presence of the TETB in SMM#2, differences between the simulated and typical actual micro-modules are as follows:

1. The simulated units have less riser wires (4 for SMM#2 compared to 12 in a micro-module) and less wafers (2 compared to about 10). These differences would tend to make the buildup of heat greater in the simulated units.

2. The simulated units include two thermocouples, but no actual transistors, which are, of course, also heat generators. This difference would tend to make the heat buildup less in the simulated units.

3. Another difference, of indeterminate effect, would be the intermingling of heat generators and heat-sensitive elements in a typical actual micro-module, compared to the simple configuration used in the simulated units.

*Thermoelectric Thermal Barrier*

1. *Design Considerations:* The design requirements were based to an extent on those specified for the binary divider micro-module being produced under the Army Micro-Module Program – in particular, the specified size, power, and temperature limitations. The power dissipated as heat in this module approaches 0.5 watt. Since the maximum allowable junction temperature of the germanium transistor used is 100°C and the maximum operating ambient temperature specified is 85°C, this 0.5 watt must be dissipated with a module internal temperature rise not greater than 15°C. According to information given in the RCA Fifth Quarterly Report mentioned above, tests had indicated that this maximum allowable rise of 15°C could be expected with only about 0.074 watt in a module with no heat sink, thus presenting a heat dissipation problem.

Accordingly, it was decided to design the simulated micro-module with a heat-generating source of 0.5 watt (two 1/4-watt resistors) and a TETB capable of holding the heat-sensitive element temperature to less than 100°C at ambient temperatures up to 85°C at 0.5 watt power dissipation.

An obvious requirement for the TETB in a micro-module is small size, not only for dimensional compatibility but also economy of thermoelectric materials. Another requirement is low Peltier current for economy of operation, low additional heat dissipation, and less chance of interaction with the functional circuitry. From previous experimentation, it was known that only a few amperes would suffice for the intended application.

2. *Material:* The best available thermoelectric materials on hand at the start of the investigation period were P and N type bismuth telluride ($Bi_2Te_3$). Characteristic data furnished by the supplier (Ohio Semiconductor, Inc., Columbus, Ohio) are as follows:

| | P Type | N Type |
|---|---|---|
| S = Seebeck coefficient (microvolts per °K) | +188 | −156 |
| k = Thermal conductivity (watts per cm per °K) | $2.5 \times 10^{-2}$ | $1.57 \times 10^{-2}$ |
| $\rho$ = Resistivity (ohm-cm) | $0.95 \times 10^{-3}$ | $0.77 \times 10^{-3}$ |
| Z = Figure of merit ($°K^{-1}$) | $2.11 \times 10^{-3}$ | $2.02 \times 10^{-3}$ |

3. *Form:* Slugs of P and N type semiconductor material were prepared on the basis of design considerations mentioned previously and available thermoelectric material. Each slug was about 0.3" in depth by 0.15" in width by 1/16" in height. The cross-sectional dimensions were selected to fit a micro-wafer. The height was chosen more or less arbitrarily, with the prime consideration being a need to limit the increase in total micro-module height. To some extent, results of previous experimentation were also considered.

The influence of the length to area (1/A) ratio can be seen from Eq. (7) in the Appendix. It will be noted that a large 1/A is better from the standpoint of low back-thermal flow ($Q_k$), but a small 1/A results in a lower Joule heating loss ($Q_j$) in the thermoelements. Also, too small an area A can lead to higher contact resistance, further increasing Joule heating. Optimum design calls for a compromise in the 1/A ratio.

4. *Fabrication of Thermoelectric Thermal Barrier:* The bismuth telluride material was obtained from the supplier in rod form, 1/2" in diameter by several inches in length. These were cut to size by sandblasting with an S. S. White Model C Industrial "Airbrasive" unit. This method was employed because the amount of heat and stress applied to the brittle slugs is less than when a diamond saw is used. In an attempt to keep junction (i.e., contact) resistances low, the following technique was employed. Both ends of the slugs were tinned with pure lead, using an ultrasonic soldering iron. A copper tab, 0.015" thick, was soldered conventionally with 60/40 tin-lead solder to the top ends of the P and N slugs to form the cold junction. Tabs of the same material were joined to the bottom ends. Wire leads (0.032" dia.) for carrying the Peltier current were soldered to these tabs. The single Peltier couple thus formed was attached to a micro-module wafer with Duco cement (see Fig. 2).

*Assembly of Simulated Micro-Module*

The various elements described above and shown in Fig. 1 and 2(b) were positioned in a rubber mold and encapsulated in Emerson-Cummings "Stycast" 2651 black epoxy to form the completed micro-module (see Fig. 2(a)).

## EVALUATION PROCEDURE

*Mounting*

With one exception, the simulated micro-modules were connected to the test printed wiring board shown in Fig. 3. (Reference is made to section under "Discussion" regarding exception.) This board is of a design used by RCA as a mount during heat transfer studies under the Army Micro-Module Program. The board was mounted, in turn, on a block of wood to confine the "conductive" heat sink to the printed wiring board and attached leads only. Small alligator clips were used to connect power leads to the printed wiring board to limit conductive heat transfer. Use of the printed wiring board in its original form resulted in a small air gap between the bottom of the simulated micro-modules and the board. Prior to Experimental Run 13, terminal area changes were made in the board which permitted SMM#2 to rest directly on the board to improve heat transfer. Also, the SMM#2 was bonded to the terminal board with a thin layer of epoxy. During Run 13 each end of the printed wiring board rested on a 4" x 6" x 2" aluminum chassis; a layer of silicone grease was used between the contacting surfaces to improve heat transfer.

*Test Circuit and Equipment*

The test circuit is depicted in Fig. 4. Also indicated is the test equipment used. Voltages and currents were measured on D'Arsonval meters for which correction factors were

determined later. Accuracy of temperature measurement was within about ±1°C. Resistances of the Peltier device and of the simulated micro-module heater circuit were measured with a Keithley Model 502 Milliohmmeter.

The power supply available for the TETB current had a high ripple at the voltages and currents supplied during this investigation. Measured values included 34% at 0.5 amperes, 14% at 2.5 amperes, and 9% at 5 amperes. (See Appendix for comments on effects and tolerable amount of ripple in Peltier couple power supplies.) The heat-generating element power supply ripple was of the order of 0.01%, too low to produce noticeable experimental measurement error.

During the transient Runs 10 and 11, a time lag of up to about one-half minute was introduced in reading the various instruments, so the times shown in the "Results" section of this report are approximations.

Test Procedures

Summary of Test Runs

| Run* | Tested Simulated Micro-Module | Nominal Ambient Temp (°C) | Printed Wiring Mount | Procedure | Purpose |
|---|---|---|---|---|---|
| 1 | #1 (without TETB) | Room | None | A | To determine internal temperature conditions at various heater dissipation levels, for comparison purposes. |
| 2 | #1 (without TETB) | Room | Used | A (0, 0.5 watt only) | Similar to above, but with printed wiring mount, such as used by RCA, to show effect of mount. |
| 3 | #1 (without TETB) | 85 | Used | A | Similar to Run 1, to show effect of higher ambient temperature. |
| 5 | #2 (with TETB) | Room | Used | A (TETB off) | Similar to Run 1 |
| 8 | #2 (with TETB) | 85 | Used | A (TETB off) | Similar to Run 3 |
| 4 | #2 (with TETB) | Room | Used | B | To show effect of various Peltier currents, with zero heater dissipation. |
| 7 | #2 (with TETB) | 85 | Used | B | Similar to Run 4, but to show added effect of higher ambient temperature. |

*NOTE: Runs are listed in convenient order for comparison, but were actually performed in the numerical order indicated to expedite testing.

## Summary of Test Runs (Cont)

| Run* | Tested Simulated Micro-Module | Nominal Ambient Temp (°C) | Printed Wiring Mount | Procedure | Purpose |
|---|---|---|---|---|---|
| 6 | #2 (with TETB) | Room | Used | B | Similar to Run 4, but with 0.5 watt heater dissipation. (Heater and initial Peltier currents turned on simultaneously.) |
| 9 | #2 (with TETB) | 85 | Used | B | Similar to Run 7, but with 0.5 watt heater dissipation. (Heater and initial Peltier currents turned on simultaneously.) |
| 10 | #2 (with TETB) | Room | Used | C | To show dynamic effect of turning on Peltier current after 0.5 watt heater dissipation has produced equilibrium conditions. |
| 11 | #2 (with TETB) | 95** | Used | C | Similar to Run 10 but at higher ambient temperature. |
| 12 | #2 (with TETB) | 95** | Used | D | Extension of Run 11, to show minimum Peltier current necessary to maintain heat-sensitive element at 100 °C. (First set of readings for Run 12 is identical to last set for Run 11.) |
| 13 | #2 (with TETB) | 95** | Used (Modified) | C | To show effect of improving heat transfer from SMM#2. |

*NOTE: Runs are listed in convenient order for comparison, but were actually performed in the numerical order indicated to expedite testing.

**See "Discussion" regarding reason for increase in ambient temperature.

1. *Procedure A*

a. With heater and Peltier voltages off, measure ambient temperature ($T_a$), heat-sensitive zone temperature ($T_{hs}$), and heat-generating zone temperature ($T_{hgm}$). Also measure heat-generating element resistance ($R_{hg}$), and, for SMM#2, Peltier device resistance ($R_p$) also, unless run starts in heated oven.

b. Apply heater voltage ($V_{hg}$) to heat-generating element sufficient to produce 0.1 watt power dissipation ($P_{hg}$). (Use $V_{hg} = (P_{hg}R_{hg})^{1/2}$ and check with $P_{hg} = V_{hg}I_{hg}$, where $I_{hg}$ is heater current.)

c. Record $T_a$, $T_{hs}$, $T_{hgm}$, $V_{hg}$, $I_{hg}$, and time at intervals, until "practical" thermal equilibrium is attained. If $T_{hs}$ and $T_{hgm}$ remain constant to ±0.5°C over a 5-minute interval, consider this as "practical" thermal equilibrium. (In Runs 13 and 14 a less stable oven was used; if $T_{hs}$ and $T_{hgm}$ remained constant to ±1°C, this was considered to indicate "practical" equilibrium.)

d. Repeat steps b and c with $P_{hg} = 0.3$ watt.

e. Repeat steps b and c with $P_{hg} = 0.5$ watt.

2. *Procedure B*

a. Same as for Procedure A, step a.

b. Same as for Procedure A, step b, to produce desired power dissipation. (Omit this step for zero heat load runs.)

c. Simultaneously with step b above, adjust Peltier power supply voltage ($V_p$) to obtain initial Peltier current ($I_p$) of 0.5 ampere.

d. Same as for Procedure A, step c, except measure $V_p$ and $I_p$ also.

e. Repeat steps c and d above at increased Peltier currents in increments of (usually) 0.5 ampere (i.e., 1.0, 1.5, 2.0, 2.5, etc.). (Note: At currents higher than about 3.5 amperes, $T_{hs}$ began to increase: run was stopped after 3.0 ampere step.)

3. *Procedure C*

a. Same as for Procedure A, step a.

b. Same as for Procedure A, steps b and c, to obtain thermal equilibrium at 0.5 watt dissipation.

c. Apply Peltier current, adjusting voltage rapidly to obtain $I_p$ of 2.5 amperes.

d. Same as for Procedure A, step c, except record $V_p$ and $I_p$ also. (Note: In Runs 10 and 11, a rapid series of readings were made during the transient periods.)

4. *Procedure D*

a. At end of Run 11 (performed in accordance with Procedure C at 95°C ambient and $P_{hg} = 0.5$ watt), the Peltier current $I_p$ was 2.5 amperes.

b. $I_p$ was decreased in trial increments, as required, to permit heat-sensitive zone temperature $T_{hs}$ to reach an equilibrium condition of 100°C (determined by the method of Procedure A, step c, with $V_p$ and $I_p$ also being measured.)

## RESULTS

1. Test results are presented in the figures and tables. The calculated temperature differences $\Delta T_z$ ($\doteq T_{hgm} - T_{hs}$) presented in the tables are not the usual temperature differences between the hot and cold junctions ($\Delta T = T_h - T_c$) normally discussed in the literature.

2. The measured resistance $R_p$ of the Peltier couple (including resistances of thermoelements, contacts at junctions, and directly associated leads) was about 0.0052 ohm.

3. To obtain an indication of the electrical power required for TETB operation, Eq. (18) of the Appendix was employed to calculate powers corresponding to various Peltier currents, using measured values of $R_p$ and $\Delta T_z$ for typical runs. For Run 9, these powers are tabulated in Table III. Since $T_{hgm} - T_{hs}$ is not necessarily equal to $T_h - T_c$, the calculated powers shown probably differ somewhat from the true values.

## DISCUSSION

1. *Internal Temperature Conditions Without Operation of TETB (Runs 1, 3, 5 and 8):* Temperature conditions within simulated micro-modules operating without thermoelectric thermal barrier protection are shown in Fig. 5 and Table I. (Reference to Fig. 13 and the Appendix will also facilitate understanding of this discussion.) Comparative data are presented for SMM#1 (no TETB) and SMM#2 (with TETB not functioning) under several conditions of ambient temperature $T_a$ and heat-generating element power dissipation. As this power dissipation (hence, heat generation) is increased, the heat-generating zone temperature $T_{hgm}$ increases linearly. Curves for the two units do not coincide under given conditions because of individual structural differences; for example, SMM#2 has heat conducting TETB power leads, which would tend to keep its temperature lower.

With power increase, the heat-sensitive zone temperature $T_{hs}$ and the temperature differential $\Delta T_z = T_{hgm} - T_{hs}$ also increase almost linearly (as expected from elementary heat transfer theory involving application of the Fourier equation $Q = K\Delta T$ to series composite structures). The temperature differentials for both units are of the same order of magnitude for given ambient temperature and heat generator dissipation conditions, indicating that insertion of the TETB does not appreciably change the *overall* thermal conductivity between the two zones.

2. *Effect of TETB (Runs 4, 6, 7, 9 and 12):* The effect of the functioning TETB on the internal temperatures of SMM#2 is shown in Fig. 6 and Table II, which give equilibrium values of $T_{hs}$ and $T_{hgm}$ measured at various TETB currents under several ambient temperature and power dissipation conditions. (In SMM#2, $T_{hs}$ is practically identical to the cold junction temperature $T_c$ appearing in the equations in the Appendix. However, the hot junction temperature $T_h$ is not necessarily the same as $T_{hgm}$, as mentioned previously.)

At zero TETB current, $T_{hgm}$ and $T_{hs}$ in Fig. 6 are the same, of course, as the values shown in Fig. 5 for corresponding ambient temperatures and heat generator dissipation values.

Under conditions of zero heat generator dissipation and normal room ambient temperature (Run 4), $T_{hgm}$, adjusting to the surrounding thermodynamic conditions, rises nonlinearly with increasing TETB current. (The nonlinearity is traceable to the Joule heating or $I^2R$ term of Eq. (11) of the Appendix.)

The heat-sensitive zone temperature $T_{hs}$ decreases at first with TETB current increase, then rises as Joule and thermal leakage heating overtake the Peltier cooling. (See Eq. (7).) The minimum portions of the $T_{hs}$ curves are rather flat; the lowest temperatures occur near 4 amperes.

Referring to the no load runs, $T_{hgm}$ remains closer than $T_{hs}$ to the ambient temperature initially because the lead wires provide better thermal conductance between the heat-generating zone and the surrounding air.

Similar behavior of temperatures versus TETB current (note parallelism of curves) occurs at higher heat generator dissipation and/or higher ambient temperatures, except, of course, that the actual temperatures are higher because of the additional heat loads. (With combined heat generator loading and Peltier operation, the change in $T_{hs}$ (or $T_{hgm}$) from $T_a$ is equal to the algebraic sum of the corresponding changes due to loading alone plus Peltier operation alone.) Another effect of the heat generator load is additional separation of $T_{hgm}$ and $T_{hs}$ by a constant amount. (See Eq. (8) and (12) and Fig. 13.)

The temperature differential $\Delta T_z$ for the high ambient temperature sets of curves is somewhat larger than for the corresponding room ambient sets, possibly as a result of material parameter changes with temperature.

It will be noted in Fig. 5 (or 6, at $I_p = 0$) that, even at 0.5 watt dissipation and 85°C ambient temperature, the heat-sensitive zone did not exceed 100°C. Hence, the problem condition mentioned under "Experimental Apparatus" did not materalize. Therefore, it was decided to create this problem condition by raising the ambient temperature for subsequent high-temperature runs (12 and 13) to about 95°C. Run 12 curves, plotted on Fig. 6 for comparison with Run 9 (0.5 watt, 85°C) curves, are discussed later.

3. *Dynamic Behavior (Runs 10 and 11):* Results of Runs 10 and 11 presented in Fig. 7 show the protective effect of switching on a TETB current of 2.5 amperes after a 0.5 watt heat generator dissipation has produced thermal equilibrium conditions in SMM#2. Following application of TETB current, internal temperatures changed rapidly to within a degree or two of their new equilibrium values in less than one minute.

A TETB current of 2.5 amperes was chosen for these runs, rather than the optimum of about 3.5 to 4.0 amperes indicated by the Fig. 6 curves. Advantage was taken of the above-noted flatness of the minimum portion of the curves to obtain a large reduction in Peltier power (power was about 0.05 watt at 2.5 amperes compared to double this power at 4.0 amperes) with only a one or two degree warmer $T_{hs}$. Use of the lower current also reduces heating of the heat-generating element by the TETB and provides other advantages, as noted under "Experimental Apparatus."

Considering the 94°C curves (Run 11), it will be observed that $T_{hgm}$ rose to 114°C, which an actual 1/2 watt micro-resistor should be capable of withstanding without derating. A drop of 7°C to a final value of 96°C occurred in $T_{hs}$. For the purpose of demonstrating protection by a TETB, it would have sufficed to reduce $T_{hs}$ to the 100°C safe operating temperature for germanium transistors. The requisite TETB current for this condition was determined by Run 12, performed (with decreasing currents) immediately after Run 11. As Fig. 6 shows, approximately 1 ampere (representing about 0.01 watt of Peltier couple power) served to maintain $T_{hs}$ at 100°C. This protective effect is also depicted in Fig. 8.

One of the potential advantages of Peltier cooling over natural cooling methods is the ability to drop $T_{hs}$ below ambient temperature. (See Run 7 curve in Fig. 6.) In work on an early version of the simulated micro-module, $T_{hs}$ dropped below $T_a$ at 0.5 watt heat generator dissipation and 2.5 amperes Peltier current. However, during the present series of tests, below-ambient temperatures were not attained under these circumstances. In an attempt to realize this condition, it was decided to improve the rather limited heat transfer from SMM#2. (The printed wiring board used as a mount (see "Evaluation Procedure") is not an adequate heat sink, as indicated by the results of Runs 1 and 2 (see Note 2 of Table I), which show that internal temperatures of SMM#1 were about the same, with or without this board.) Consequently, the changes

described under "Evaluation Procedure" were made, and Run 13, similar to Run 11, was performed. Significant results are compared with Run 11 data in Table IV. The lower values of $T_{hgm} - T_a$ for Run 13, despite a 0.02 watt higher power, indicate that heat transfer was improved. While the desired "below ambient" condition was not attained, $T_{hs}$ was reduced to about ambient temperature with a 2.5 ampere Peltier current.

## CONCLUSIONS

Experimental results with a simulated micro-module operating at temperatures between 25°C and 95°C indicate that it is possible under certain circumstances to protect a heat-sensitive element from a heat-generating element within the same micro-module by means of a small, low current Peltier device (thermoelectric thermal barrier) built directly into the micro-module between these elements.

## RECOMMENDATIONS

1. It is recommended that internal work be continued on the thermoelectric thermal barrier to demonstrate its practical application. This would be the next step towards its establishment as an acceptable heat transfer means. This work would utilize Peltier devices in microelement form soon to be obtained from a contract based on the reported investigation. (Signal Corps Contract No. DA36-039 sc-89212 with Melpar, Inc., Falls Church, Va.) These devices would be incorporated into actual micro-modules containing functional circuitry and employing structural refinements to improve heat transfer characteristics.

2. In conjunction with the above-recommended work directed toward specific applications, research is recommended on associated design and fabrication techniques. Possible avenues of investigation include thin film thermoelements, reduction of junction resistance, reduction of leakage heat flow $Q_k$, use of pulsed Peltier current, and use of a combination of cooling and power generating thermoelectric couples (the latter employing "waste" heat from the heat-generating element).

## SELECTED REFERENCES

*Books*


1. Ioffe, A. F., *Semiconductor Thermoelements and Thermoelectric Cooling* (Infosearch Limited, London; 1957).

2. Kaye, J. & Welsh, J. A., *Direct Conversion of Heat to Electricity* (M.I.T. Special Summer Program; July 1959).

3. Shive, J. N., *Semiconductor Devices* (Van Nostrand, Princeton; 1959).

4. Ioffe, A. F., *Physics of Semiconductors* (Academic Press, N. Y.; 1960).

5. Egli, P. H., *Thermoelectricity* (Wiley, N. Y.; 1960).

6. Cadoff, I. B. & Miller, E., *Thermoelectric Materials and Devices* (Reinhold, N. Y.; 1960).

   (NOTE: This collection includes such informative chapters as "Thermoelectric Phenomena" by N. Fuschillo; "Calculation of Efficiency of Thermoelectric Devices" by B. Sherman, R. R. Heikes and R. W. Ure, Jr.; and "Design Calculations for Peltier Cooling" by R. H. Vought.)

7. Goldsmid, H. G., *Applications of Thermoelectricity* (Wiley, N. Y.; Methuen, London; 1960).

8. Zemansky, Mark W., *Heat and Thermodynamics* (McGraw-Hill, N. Y.; 1948).

9. Schneider, P. J., *Conduction Heat Transfer* (Addison-Wesley, Cambridge, Mass.; 1955).

10. Jakob, M. & Hawkins, G. A., *Elements of Heat Transfer* (Wiley, N. Y.; 1957).

*Periodicals*

11. Domenicali, C. A., "Irreversible Thermodynamics of Thermoelectricity," Revs. Modern Phys. (April 1954).

12. Burshtein, A. I., "An Investigation of the Steady-State Heat Flow Through a Current-Carrying Conductor," *Soviet Phys.-Tech. Phys.*, (Am. Inst. of Physics Translation; July 1957).

13. Harman, T. C., Paris, B., Miller, S. E., & Goering, H. L., "Preparation and Some Physical Properties of $Bi_2Te_3$, $Sb_2Te_3$, and $As_2Te_3$," *J. Phys. Chem. Solids*, Vol. 2, No. 3 (1957).

14. Shilliday, T. S., "Performance of Composite Peltier Junctions of $Bi_2Te_3$," *J. Appl. Phys.* (September 1957).

15. Jaumot, F. E., Jr., "Thermoelectric Effects," *Proceedings of the IRE* (March 1958).

16. Eichhorn, R. L., "Thermoelectric Refrigeration," *Refrigerating Engineering* (June 1958).

17. Kronsbein, J. and Hartsaw, W. O., "The Peltier Effect," *Refrigerating Engineering* (September 1958).

18. "Thermoelectric Cooling Guide," *Refrigerating Engineering* (September 1958).

19. Lindenblad, N. E., "Thermoelectric Heat Pumping," *Electrical Engineering* (September 1958).

20. Joffe, A. F., "The Revival of Thermoelectricity," *Scientific American* (November 1958).

21. Lackey, R. S., Meess, J. D., and Somers, E. V., "Applications of Thermoelectric Cooling and Heating," *Refrigerating Engineering* (December 1958).

22. Heinicke, J. B., "Design and Performance of a Thermoelectric Refrigerator," *Refrigerating Engineering* (February 1959).

23. Danielson, W. R., "Temperature-Controlled Chamber Using Thermoelectric Cooling," *Refrigerating Engineering* (February 1959).

24. Celent, C., "Thermoelectricity–State of the Art," *Electronic Industries* (July 1959).

25. "Peltier Thermostating," *Electronic Industries* (July 1959).

26. Benedict, R. P., "Thermoelectric Effects," *Electrical Manufacturing* (February 1960).

27. Parrott, J. E., "The Interpretation of the Stationary and Transient Behavior of Refrigerating Thermocouples," *Solid State Electronics* (May 1960).

28. Huck, W. V., "Thermoelectric Elements for Heat-Pump Devices," *Electrical Manufacturing* (May 1960).

29. Taylor, J. and Mulicia, A., "Thermoelectric Coolers for Electronic Components," *Electrical Manufacturing* (May 1960).

30. Angello, S. J., "Recent Progress in Thermoelectricity," *Electrical Engineering* (May 1960).

31. Lougher, H. H., "Measurement of the Parameters in the Thermoelectric Figure of Merit," *Electrical Engineering* (May 1960).

32. Sickert, R. G., "A Thermoelectric Refrigerating System for Submarines," *Electrical Engineering* (May 1960).

33. Wright, W. L., "Thermoelectric Refrigeration," *Electrical Engineering* (May 1960).

34. Alfonso, N. and Milnes, A. G., "Transient Response and Ripple Effects in Thermoelectric Cooling Cells," *Electrical Engineering* (June 1960).

35. Hudelson, G. D., "Thermoelectric Air Conditioning of Totally Inclosed Environments," *Electrical Engineering* (June 1960).

36. Donahoe, F. J., "Theoretical Bound on the Thermoelectric Figure of Merit," *Electrical Engineering* (June 1960).

37. Scofield, D. W., Taylor, P. F. and Staebler, L. A., "A Comparative Study of the Manufacturing Costs of Thermoelectric and Mechanical Refrigerating Systems," *ASHRAE Journal* (July 1960).

38. Sherman, B., Heikes, R. R., and Ure, R. W., Jr., "Calculation of Efficiency of Thermoelectric Devices," *J. Appl. Phys.* (January 1961).

39. Snyder, P. E., "Chemistry of Thermoelectric Materials," *Chem. Eng. News* (March 13, 1961).

40. Mette, H., "Power Generation and Heat Pumping by Thermoelectric Phenomena," *The Solid State Journal* (May 1961).

*Contractual Reports*

41. Miller, E., Selikson, B., Cadoff, I., and Telkes, M., "Research on Peltier Effect Cooling," Final Report, U. S. Army Contr. No. DA36-039 SC-71133, New York University (January 1957).

42. Gray, P. E. et al., "Theoretical and Experimental Research in Thermoelectricity," Scientific Report #1, AFCRC-TN-60-125, USAF Contr. No. AF19(604)-4153, M.I.T. (December 1959).

43. Martz, E. F., Sickert, R. G., and Wolfert, E. R., "Type I Thermoelectric Temperature Controlled Chambers," Final Development Report, U. S. Navy Contr. No. NObsr-77617, Whirlpool Corporation (August 1960).

44. Carey, B., and Marlow, R., "Peltier Cooling of Semiconductor Components," Final Technical Report, U. S. Navy Contr. No. NObsr-81204, Texas Instruments Inc. (June 1961).

*Government Publications*

45. Stauss et al., Issues of "Status Report on Thermoelectricity," Naval Research Laboratories Memorandum Reports, beginning February 1959.

46. Johnson, A. D., "Thermoelectric Phenomena," Air Force Cambridge Research Center Report No. AFCRC-TR-59-362 (December 1959).

47. Welsh, J. P. and Walsh, T. W., "Handbook of Methods of Cooling Semiconductor Devices," Rome Air Development Center Report No. RADC-TR-60-22 (August 1960).

48. Moorhead, J. G., "Cooling Large Electronics Packages," Diamond Ordnance Fuze Laboratories Report No. TR-882 (January 1961).

*Proceedings*

49. Whirlpool Corporation "Proceedings – Whirlpool Thermoelectric Symposium, Washington, D. C." (October 21, 1959).

*Manufacturer's Literature*

50. Merck, "Thermoelectric Materials."

*Miscellaneous*

51. Hoxton, L. G., "Thermoelectricity," *McGraw-Hill Encyclopedia of Science and Technology*, Vol. 13 (1960).

TABLE I

INTERNAL TEMPERATURES IN SIMULATED MICRO-MODULES
(THERMOELECTRIC THERMAL BARRIER INOPERATIVE)

| Heat-Generating Element Power (watts) | SMM #1 – Without TETB | | | | | | SMM #2 – With TETB (Inoperative) | | | | | |
|---|---|---|---|---|---|---|---|---|---|---|---|---|
| | Amb. Temp. 25 °C (Run 1) | | | Amb. Temp. 85 °C (Run 3) | | | Amb. Temp. 25 °C (Run 5) | | | Amp. Temp. 85 °C (Run 8) | | |
| | $T_{hgm}$ (°C) | $T_{hs}$ (°C) | $\Delta T_z$ (°C) | $T_{hgm}$ (°C) | $T_{hs}$ (°C) | $\Delta T_z$ (°C) | $T_{hgm}$ (°C) | $T_{hs}$ (°C) | $\Delta T_z$ (°C) | $T_{hgm}$ (°C) | $T_{hs}$ (°C) | $\Delta T_z$ (°C) |
| 0 | 24.4 | 24.3 | 0.1 | 83.0 | 82.3 | 0.7 | 23.9 | 23.9 | 0 | 83.9 | 83.9 | 0 |
| 0.10 | 30.0 | 27.5 | 2.5 | 87.5 | 85.7 | 1.8 | 28.9 | 27.2 | 1.7 | 87.5 | 85.8 | 1.7 |
| 0.29 | 41.8 | 35.8 | 6.0 | 97.5 | 91.5 | 6.0 | 37.4 | 32.8 | 4.6 | 96.1 | 90.8 | 5.3 |
| 0.47 | 50.0 | 40.5 | 9.5 | 106.2 | 97.5 | 8.7 | 47.3 | 39.2 | 8.1 | 104.2 | 95.8 | 8.4 |

NOTES:
1. See "Symbols" (Appendix) for definitions of $T_{hgm}$, $T_{hs}$ and $\Delta T_z$.
2. All runs, except Run 1, were made using printed circuit mount. A short run (Run 2) was made with SMM #1 on the printed circuit mount at 25 °C ambient temperature and with a 0.5 watt heat-generating element power. Measurements of $T_{hgm}$ and $T_{hs}$ were only about 0.5 °C less than corresponding readings shown for Run 1 under the same conditions.
3. Temperature readings for Runs 1 and 5 are adjusted to correct for small, slow ambient temperature deviations from 25 °C. Similar adjustments were not made for 85 °C (nominal) runs because it was observed that simulated micro-module internal temperatures did not follow the larger, rapid fluctuations in oven temperature. Ambient temperature ranges were 86 ° to 87.5 °C for Run 3, and 85 ° to 86 °C for Run 8.
4. Heat-generating element powers shown are average values for indicated runs. Actual powers are within about 0.01 watt of nominal value.

TABLE II

EFFECT OF THERMOELECTRIC THERMAL BARRIER IN SIMULATED MICRO-MODULE #2

| Peltier Current (amp) | Heat-Generating Element Power = 0 watt | | | | | | Heat-Generating Element Power = 0.5 watt | | | | | | | | |
|---|---|---|---|---|---|---|---|---|---|---|---|---|---|---|---|
| | Amb. Temp. 25 °C (Run 4) | | | Amb. Temp. 85 °C (Run 7) | | | Amb. Temp. 25 °C (Run 6) | | | Amb. Temp. 85 °C (Run 9) | | | Amb. Temp. 93 °C (Run 12) | | |
| | $T_{hgm}$ (°C) | $T_{hs}$ (°C) | $\Delta T_z$ (°C) | $T_{hgm}$ (°C) | $T_{hs}$ (°C) | $\Delta T_z$ (°C) | $T_{hgm}$ (°C) | $T_{hs}$ (°C) | $\Delta T_z$ (°C) | $T_{hgm}$ (°C) | $T_{hs}$ (°C) | $\Delta T_z$ (°C) | $T_{hgm}$ (°C) | $T_{hs}$ (°C) | $\Delta T_z$ (°C) |
| 0 | 24.3 | 24.3 | 0 | 83.3 | 83.3 | 0 | 47.3 | 39.2 | 8.1 | 104.2 | 95.8 | 8.4 | 110.8 | 103.6 | 7.2 |
| 0.5 | 24.6 | 22.6 | 2.0 | 83.3 | 81.7 | 1.6 | 48.1 | 37.8 | 10.3 | 104.3 | 94.2 | 10.1 | 111.4 | 101.4 | 10.0 |
| 1.0 | 24.8 | 21.4 | 3.4 | 84.2 | 80.0 | 4.2 | 48.5 | 36.7 | 11.8 | 105.3 | 93.2 | 12.1 | 111.9 | 100.0 | 11.9 |
| 1.5 | 25.4 | 20.4 | 5.0 | 84.4 | 78.3 | 6.1 | 49.2 | 35.6 | 13.6 | 106.1 | 91.9 | 14.2 | 112.8 | 99.2 | 13.6 |
| 2.0 | 25.8 | 19.1 | 6.7 | 85.3 | 77.2 | 8.1 | 49.8 | 34.5 | 15.3 | 106.7 | 90.6 | 16.1 | – | – | – |
| 2.5 | 27.1 | 18.8 | 8.3 | 85.8 | 76.4 | 9.4 | 50.9 | 33.7 | 17.2 | 107.8 | 89.9 | 17.9 | 114.2 | 96.1 | 18.1 |
| 3.0 | 27.6 | 18.3 | 9.3 | 87.2 | 75.6 | 11.6 | 51.4 | 32.1 | 19.3 | 108.6 | 89.4 | 19.2 | – | – | – |
| 3.5 | 28.8 | 18.0 | 10.8 | 88.3 | 75.6 | 12.7 | 52.2 | 32.1 | 20.1 | 110.0 | 88.9 | 21.1 | – | – | – |
| 4.0 | 29.9 | 18.0 | 11.9 | 90.0 | 75.3 | 14.7 | 54.1 | 32.1 | 22.0 | 111.7 | 88.9 | 22.8 | – | – | – |
| 4.5 | – | – | – | 91.7 | 75.3 | 16.4 | 55.3 | 31.6 | 23.7 | 113.6 | 88.9 | 24.7 | – | – | – |
| 5.0 | 33.3 | 18.6 | 14.7 | 93.6 | 75.8 | 17.8 | 56.7 | 32.8 | 23.9 | 115.3 | 89.4 | 25.9 | – | – | – |

NOTES: 1. See "Symbols" (Appendix) for definitions of $T_{hgm}$, $T_{hs}$ and $\Delta T_z$.

2. Temperature readings for Runs 4 and 6 are adjusted to correct for small, slow ambient temperature deviations from 25 °C. Similar adjustments were not made for 85 °C (nominal) and 93 °C runs because it was observed that simulated micro-module internal temperatures did not follow the larger, rapid fluctuations in oven temperature. Ambient temperature ranges were 85° to 86.2 °C for Run 7, 85° to 86.3 °C for Run 9, and 93.0° to 93.5 °C for Run 12.

3. Actual heat-generating element powers were generally about 0.02 to 0.03 watt lower than the nominal 0.5 watt.

TABLE III

CALCULATED THERMOELECTRIC THERMAL BARRIER INPUT POWER

| Peltier Current (Amperes) | 0.5 | 1.0 | 1.5 | 2.0 | 2.5 | 3.0 | 3.5 | 4.0 | 4.5 | 5.0 |
|---|---|---|---|---|---|---|---|---|---|---|
| Peltier Power (Milliwatts) | 3 | 9 | 19 | 32 | 48 | 67 | 89 | 111 | 144 | 175 |

TABLE IV

EFFECT OF DESIGN MODIFICATION

| Peltier Current (amp) | Before Modification (Run 11) | | | | | After Modification (Run 13) | | | | |
|---|---|---|---|---|---|---|---|---|---|---|
| | Temperatures | | | | | Temperatures | | | | |
| | Heat-Generating Element Power (w) | $T_a$ (°C) | $T_{hgm}$ (°C) | $T_{hs}$ (°C) | $\Delta T_z$ (°C) | Heat-Generating Element Power (w) | $T_a$ (°C) | $T_{hgm}$ (°C) | $T_{hs}$ (°C) | $\Delta T_z$ (°C) |
| 0 | 0.47 | 93.5 | 110.8 | 103.1 | 7.7 | 0.49 | 96.5 | 113.6 | 106.1 | 7.5 |
| 2.5 | 0.47 | 93.5 | 114.2 | 96.1 | 18.1 | 0.49 | 98.2 | 115.8 | 98.3 | 17.5 |

NOTE: Oven temperature ($T_a$) variations were about 2°C.

VERTICAL CROSS-SECTION OF SIMULATED MICRO-MODULE
WITH THERMOELECTRIC THERMAL BARRIER

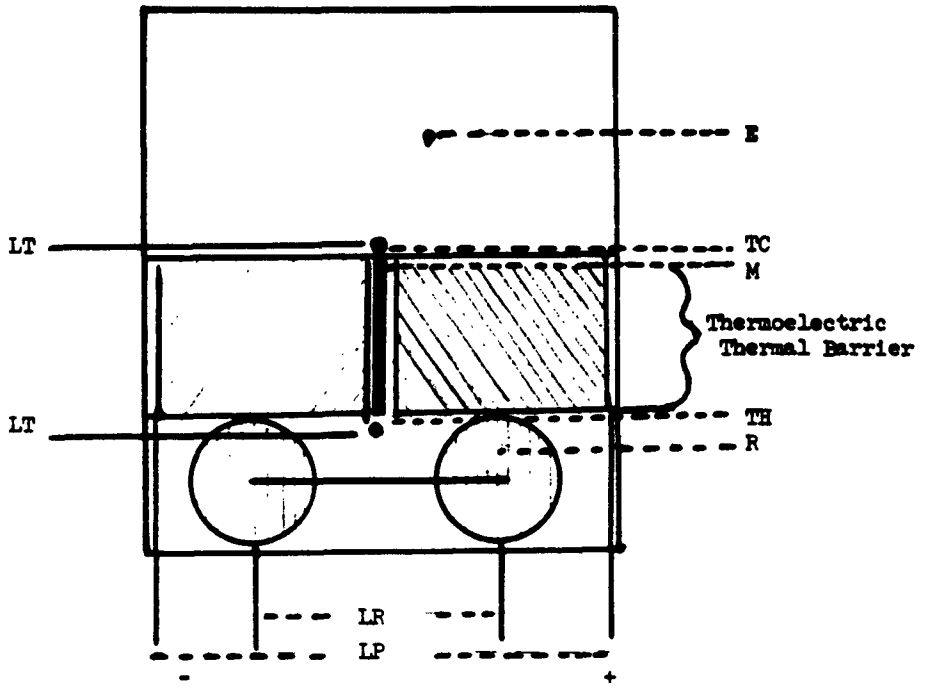


E - Epoxy encapsulant

P - P type bismuth telluride slug

N - N type bismuth telluride slug

M - Mica insulator

R - Heat generating element (resistors dissipating up to 0.5 watts)

LR - Resistor leads

LP - Peltier device leads

LT - Measuring thermocouple leads

TC - Cold zone temperature ($t_{hs}$) measuring thermocouple (Also simulates heat sensitive element)

TH - Hot zone temperature ($t_{hgm}$) measuring thermocouple.

FIGURE 1

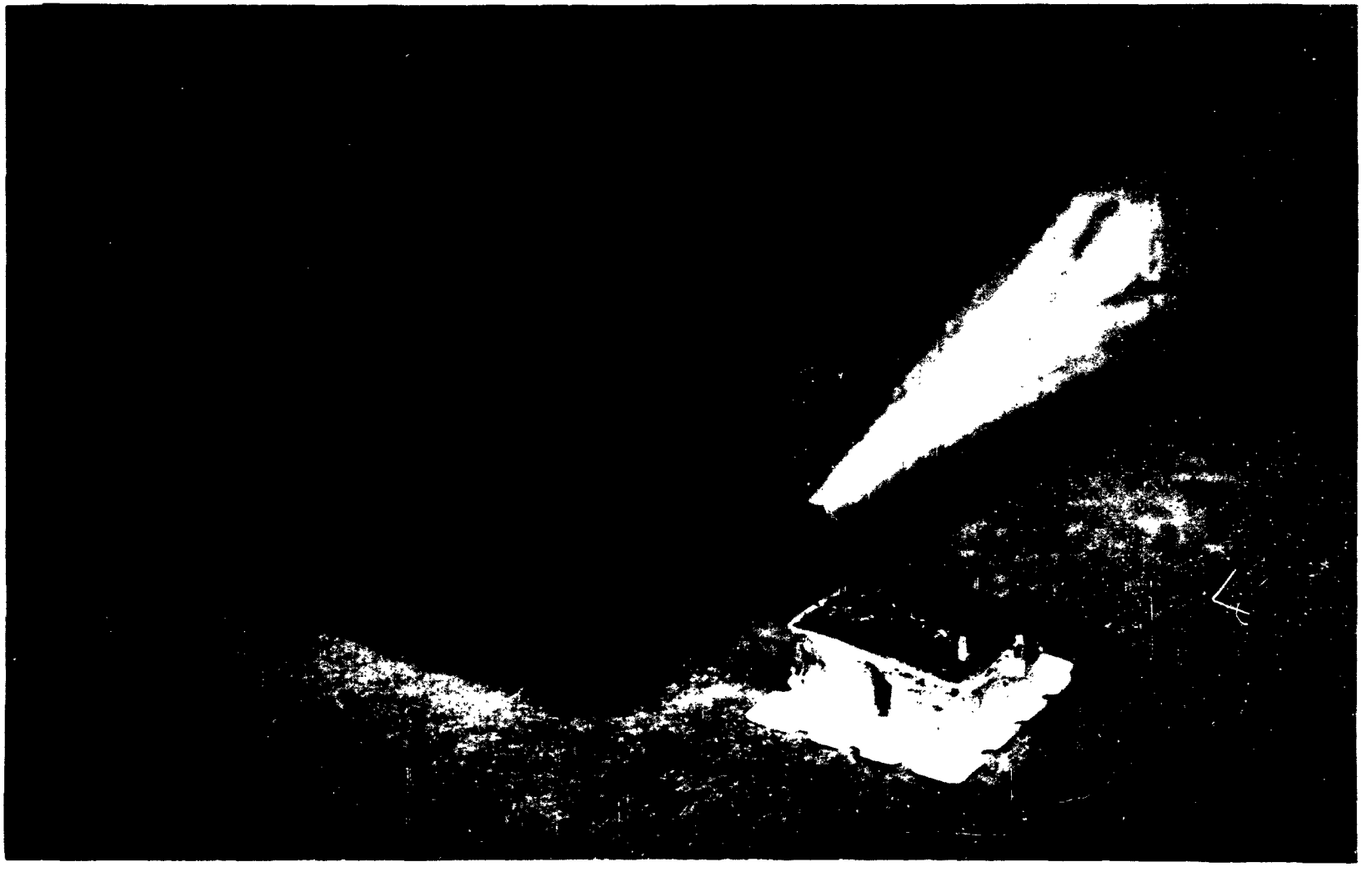

(a) (b)

Figure 2
(a) Simulated Micro-Module Containing a Thermoelectric Thermal Barrier
(b) Thermoelectric Thermal Barrier

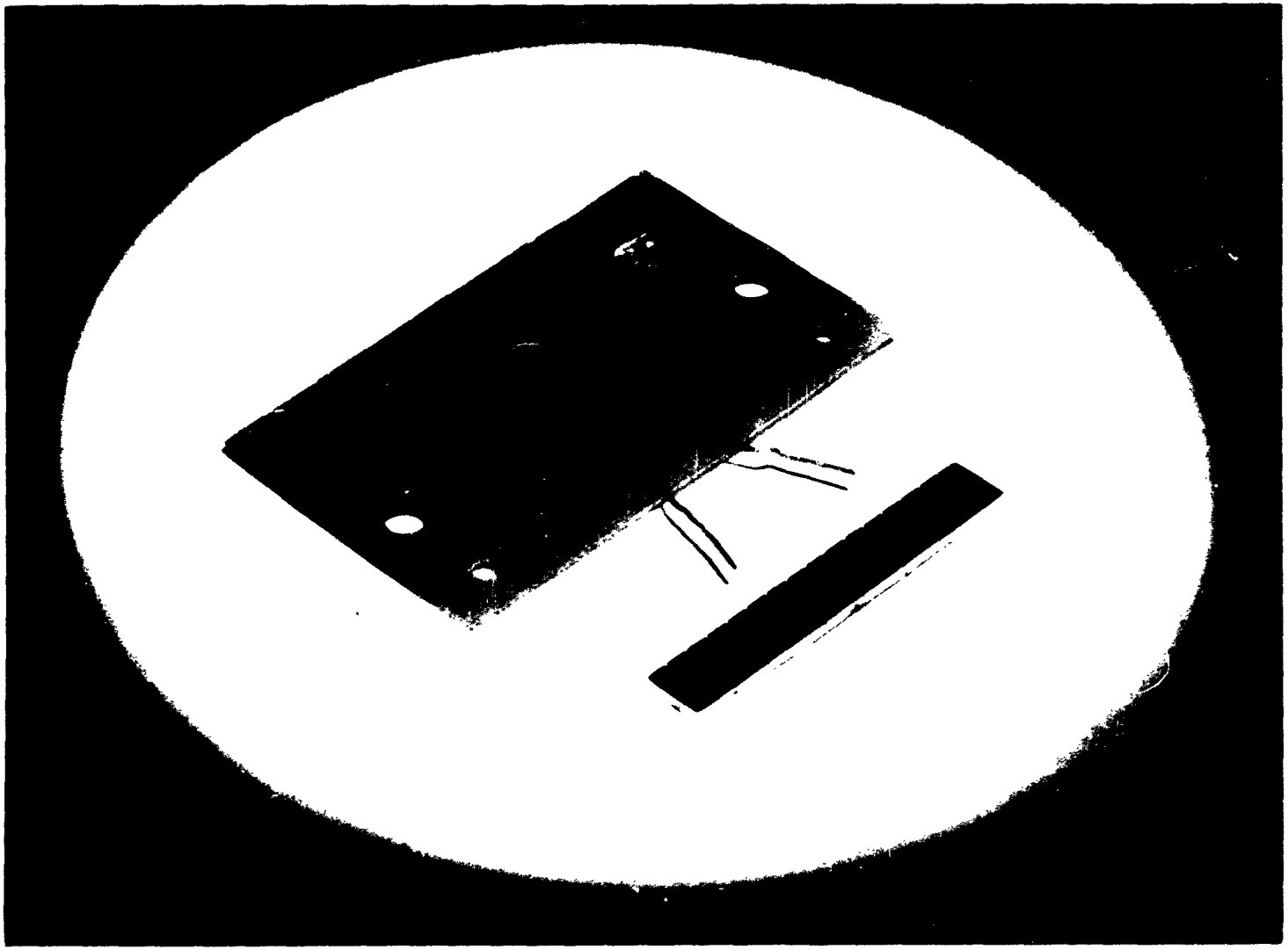

FIGURE 3
Simulated Micro-Module SMM #2 Mounted on Printed Wiring Board

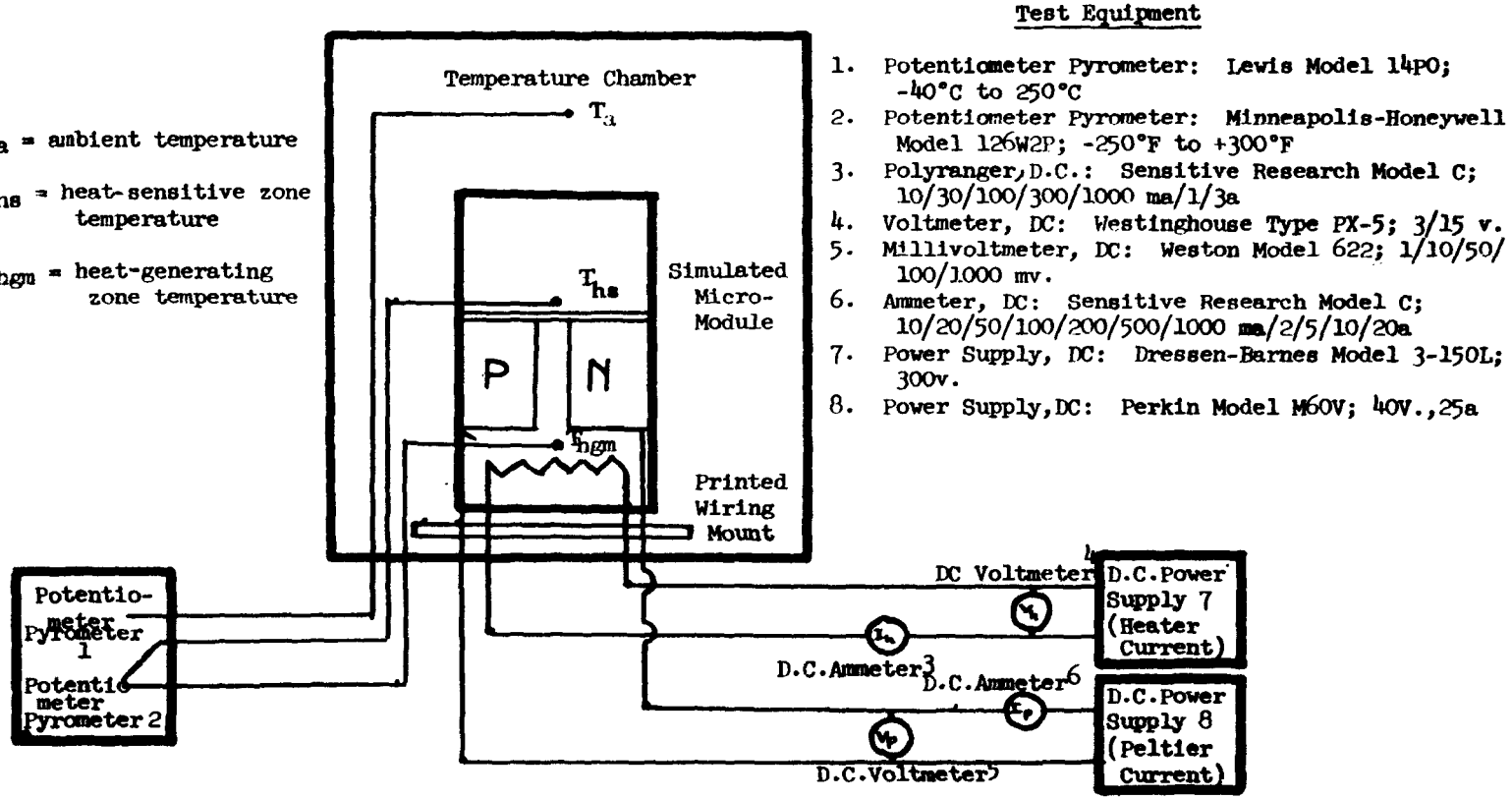


Test Equipment

1. Potentiometer Pyrometer: Lewis Model 14PO; -40°C to 250°C
2. Potentiometer Pyrometer: Minneapolis-Honeywell Model 126W2P; -250°F to +300°F
3. Polyranger, D.C.: Sensitive Research Model C; 10/30/100/300/1000 ma/1/3a
4. Voltmeter, DC: Westinghouse Type PX-5; 3/15 v.
5. Millivoltmeter, DC: Weston Model 622; 1/10/50/100/1000 mv.
6. Ammeter, DC: Sensitive Research Model C; 10/20/50/100/200/500/1000 ma/2/5/10/20a
7. Power Supply, DC: Dressen-Barnes Model 3-150L; 300v.
8. Power Supply, DC: Perkin Model M60V; 40V., 25a

FIGURE 4. TEST CIRCUIT FOR SIMULATED MICRO-MODULES

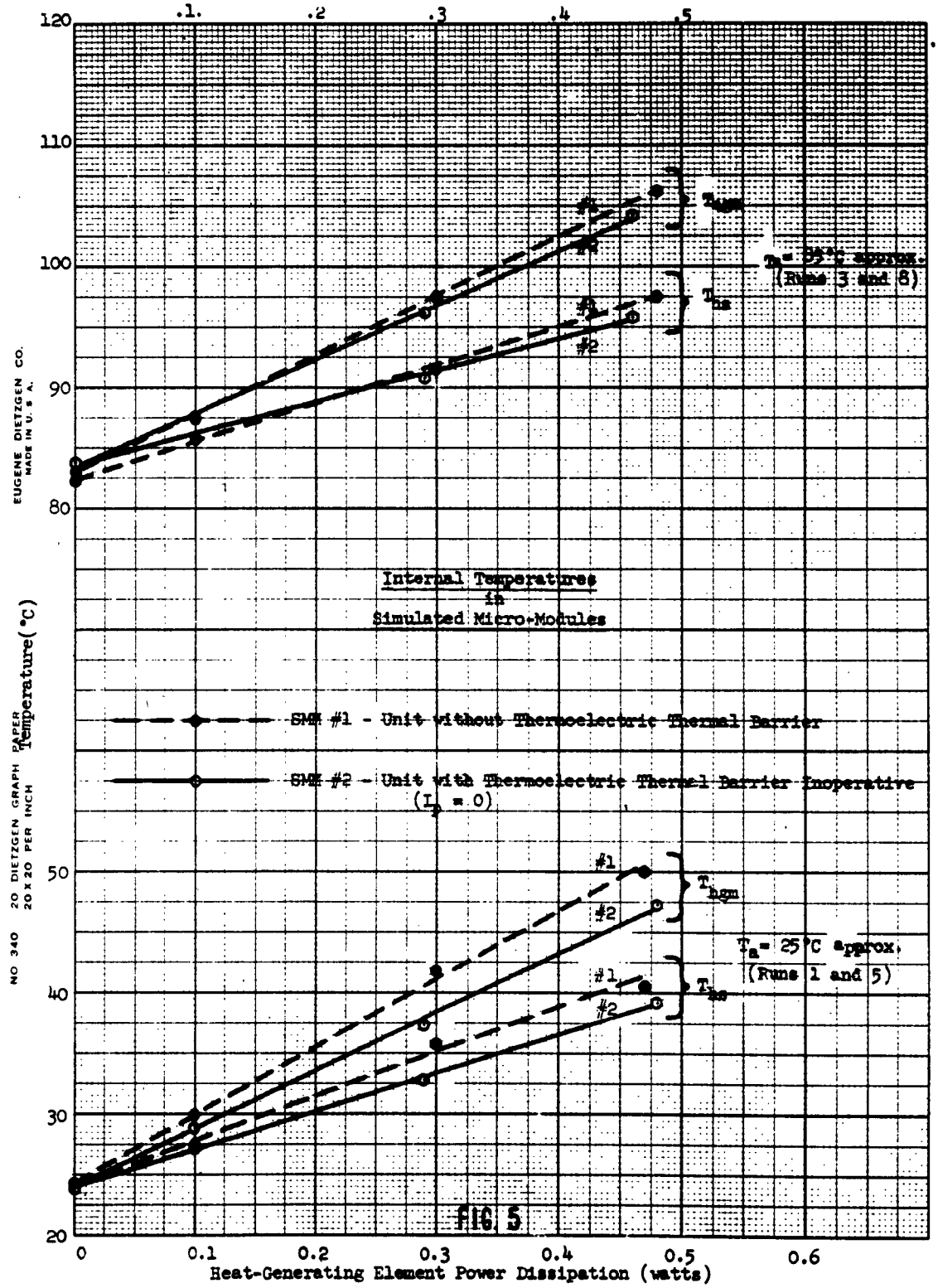
Internal Temperatures
in
Simulated Micro-Modules
SMM #1 - Unit without Thermoelectric Thermal Barrier
SMM #2 - Unit with Thermoelectric Thermal Barrier Inoperative
($I_p$ = 0)
$T_a$ = 25°C approx.
(Runs 1 and 5)
$T_a$ = 82°C approx.
(Runs 3 and 8)
$T_{hgm}$
$T_{hs}$
#1
#2
Temperature (°C)
Heat-Generating Element Power Dissipation (watts)
120
110
100
90
80
50
40
30
20
0
0.1
0.2
0.3
0.4
0.5
0.6
.1.
.2
.3
.4
.5
EUGENE DIETZGEN CO.
MADE IN U.S.A.
NO 340 20 DIETZGEN GRAPH PAPER
20 X 20 PER INCH

FIG 5

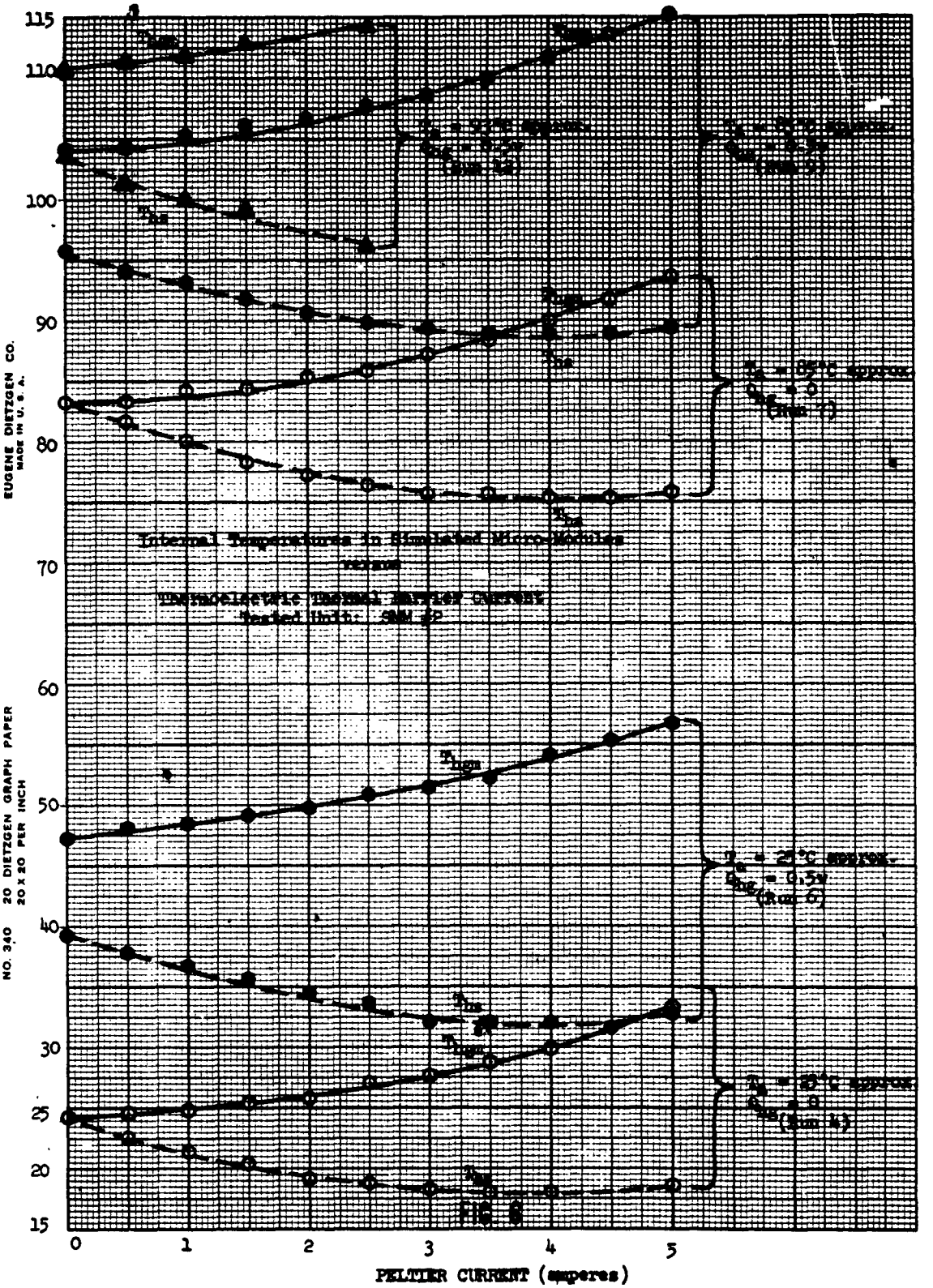
EUGENE DIETZGEN CO.
MADE IN U. S. A.
NO. 340 20 DIETZGEN GRAPH PAPER
20 X 20 PER INCH
Internal Temperatures in Shielded Micro-Modules
versus
Thermoelectric Thermal Barrier Current
Sealed Units: SMM #2
PELTIER CURRENT (amperes)
115
110
100
90
80
70
60
50
40
30
25
20
15
0
1
2
3
4
5

FIG 6

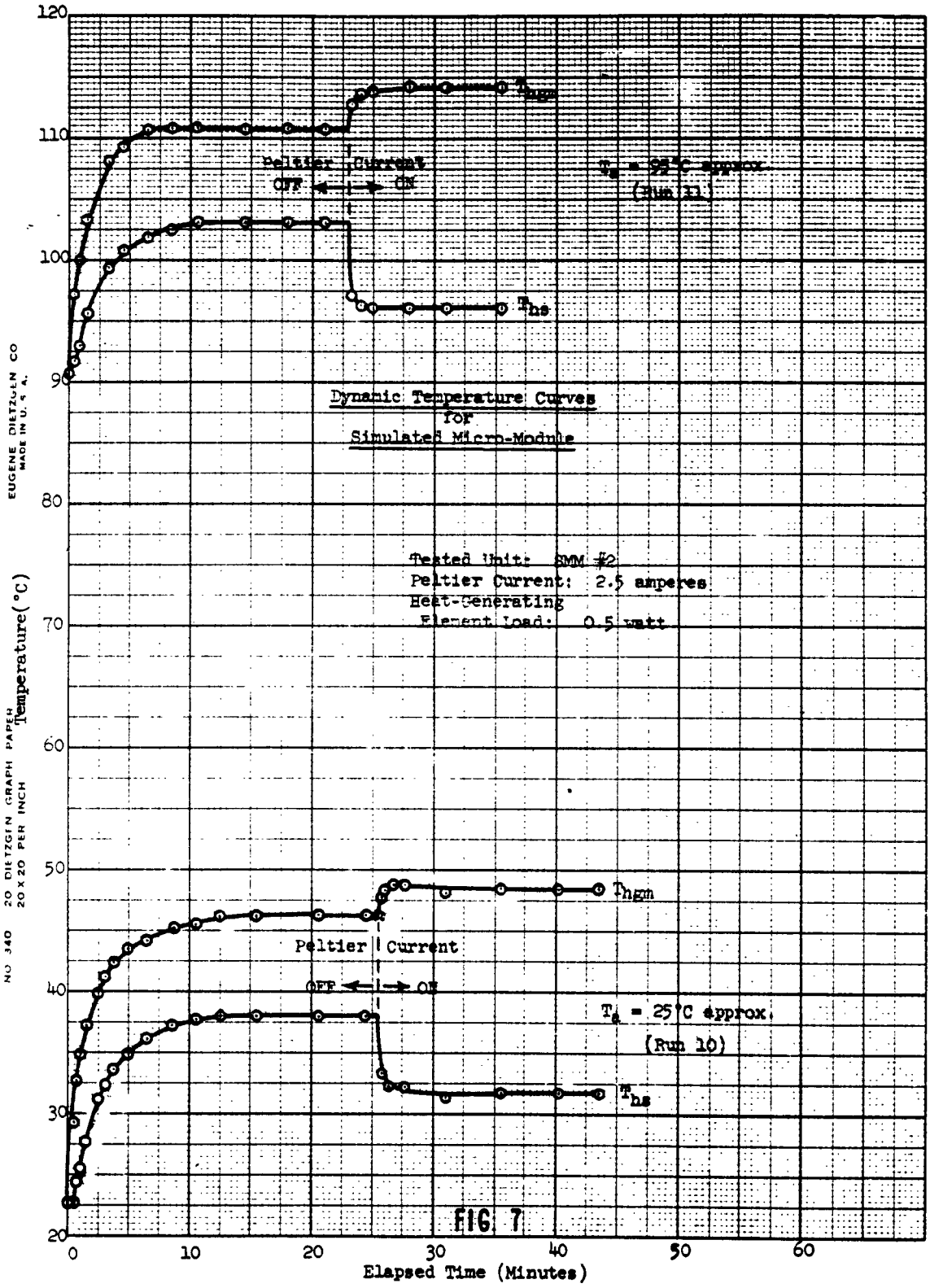
Dynamic Temperature Curves
for
Simulated Micro-Module
Tested Unit: SMM #2
Peltier Current: 2.5 amperes
Heat-Generating
Element Load: 0.5 watt
Peltier Current
OFF ON
$T_a$ = 25°C approx.
(Run 10)
$T_{hgm}$
$T_{hs}$
$T_a$ = 95°C approx.
(Run 11)
$T_{hgm}$
$T_{hs}$
Temperature (°C)
Elapsed Time (Minutes)
120
110
100
90
80
70
60
50
40
30
20
0
10
20
30
40
50
60
EUGENE DIETZGEN CO
MADE IN U.S.A.
NO 340 20 DIETZGEN GRAPH PAPER
20 X 20 PER INCH

FIG. 7

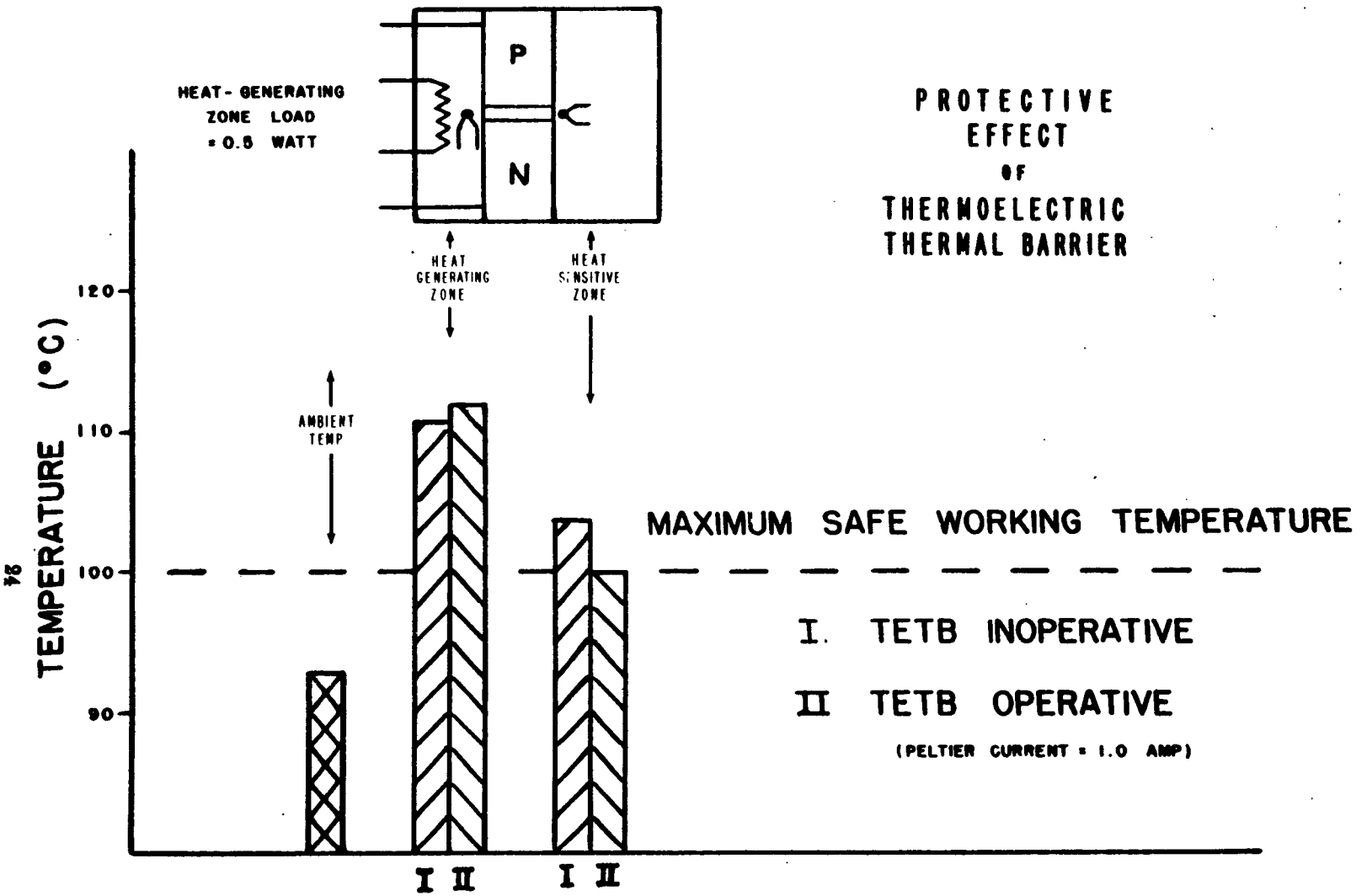
PROTECTIVE
EFFECT
OF
THERMOELECTRIC
THERMAL BARRIER
HEAT - GENERATING
ZONE LOAD
= 0.5 WATT
P
N
HEAT
GENERATING
ZONE
HEAT
SENSITIVE
ZONE
AMBIENT
TEMP
TEMPERATURE (°C)
120
110
100
90
MAXIMUM SAFE WORKING TEMPERATURE
I. TETB INOPERATIVE
II TETB OPERATIVE
(PELTIER CURRENT = 1.0 AMP)
I II
I II

FIG. 8

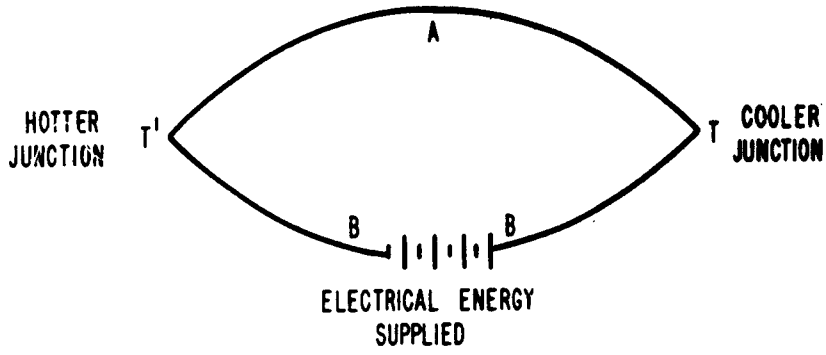


FIGURE 9 PELTIER EFFECT

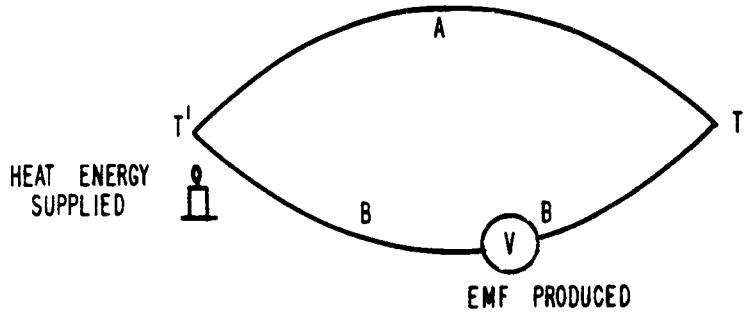


FIGURE 10 SEEBECK EFFECT

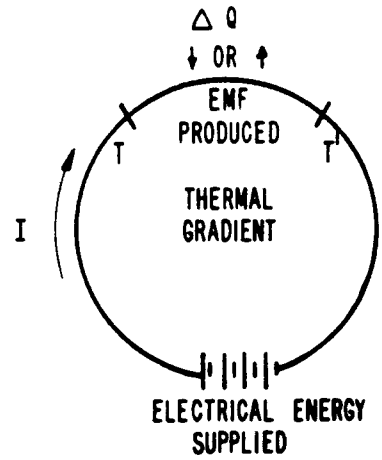


FIGURE 11 THOMSON EFFECT

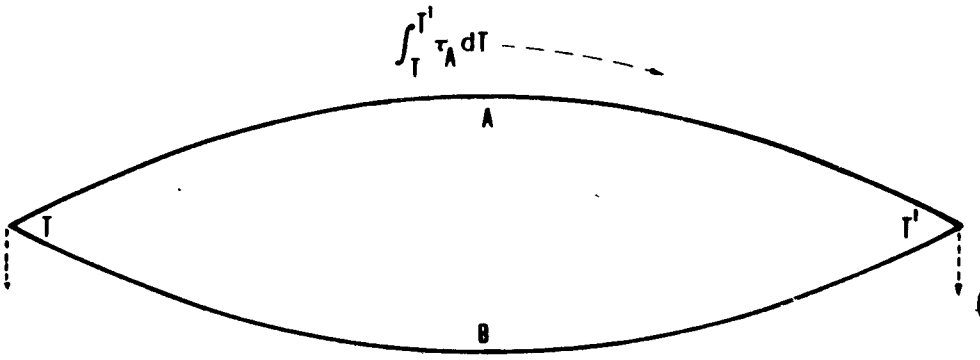




NET PELTIER EMF — NET THOMSON EMF

$$\text{SEEBECK EMF } E_S = (\pi_A - \pi_B) \text{ AT } T' - (\pi_A - \pi_B) \text{ AT } T + \int_T^{T'} \tau_A \, dT - \int_T^{T'} \tau_B \, dT$$

$$- \int_T^{T'} (S_A - S_B) \, dT$$

FIGURE 12 THERMOELECTRIC VOLTAGES

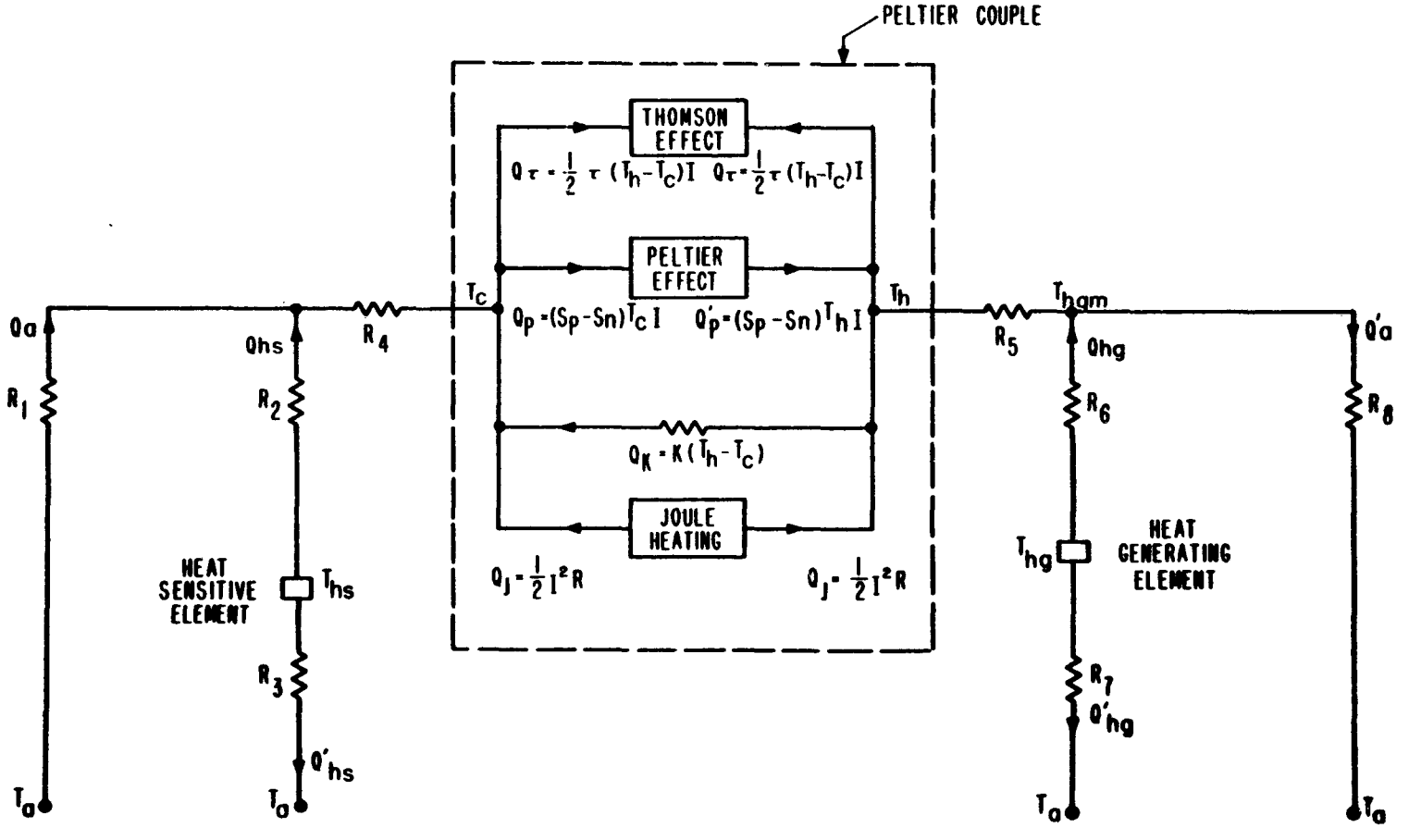


FIGURE 13
SIMPLIFIED THERMAL NETWORK FOR SIMULATED MICRO MODULE
WITH THERMOELECTRIC THERMAL BARRIER

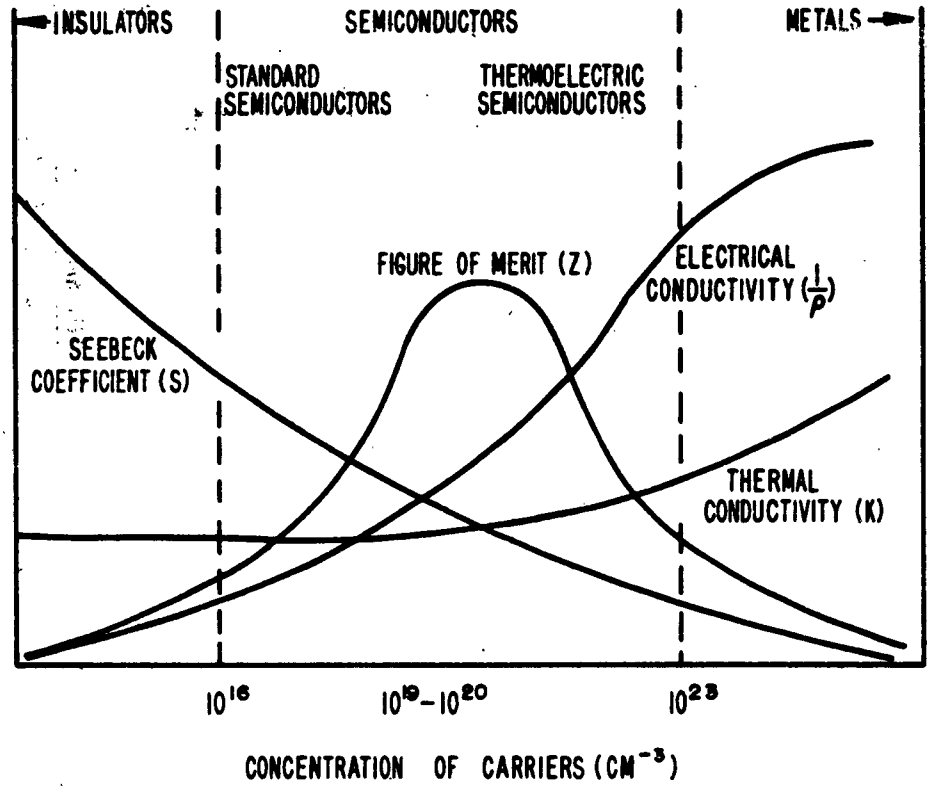


FIGURE 14 RELATIVE DEPENDENCE OF FIGURE OF MERIT Z AND CONSTITUENT PARAMETERS ON CONCENTRATION OF INTRINSIC CHARGE CARRIERS n

## APPENDIX

### 1. SYMBOLS

| | |
|---|---|
| A | Cross-sectional area of thermoelement |
| c | Specific heat capacity |
| $E_s$ | Seebeck voltage |
| I | Current |
| $I_c$ | Current for maximum coefficient of performance |
| $I_q$ | Current for maximum cooling |
| k | Thermal conductivity |
| K | Thermal conductance |
| l | Length of thermoelement |
| n | Number of charge carriers |
| Q | Rate of heat flow |
| R | Resistance |
| S | Seebeck coefficient |
| T | Temperature |
| $V_t$ | Voltage applied to Peltier couple |
| P | Power |
| X | Distance |
| Z | Figure of merit |
| $\Delta T$ | $T_h - T_c$ (difference between hot and cold junction temperatures) |
| $\Delta T_z$ | $T_{hgm} - T_{hs}$ (difference between heat generating and heat sensitive zone temperatures measured in the reported investigation) |
| $\pi$ | Peltier coefficient |
| $\rho$ | Electrical resistivity |
| $\sigma$ | Electrical conductivity |
| $\tau$ | Thomson coefficient |
| $\phi$ | Peltier current ripple factor |

*Subscripts*

| | |
|---|---|
| a | Ambient |
| A | Material A |
| B | Material B |
| c | Cold junction |
| h | Hot junction |
| hg | Heat-generating element |

*Subscripts* (Cont.)

| | |
|---|---|
| hgm | Heat-generating zone |
| hs | Heat-sensitive element or zone |
| j | Junction |
| J | Joule |
| K | Fourier |
| m | Mean |
| N | N-type semiconductor material |
| p | Peltier |
| P | P-type semiconductor material |
| $\tau$ | Thomson |

(Note: Symbols with "primes" refer to certain hot end conditions, as indicated in the "Theory" section.)

## 2. THEORY

*Introduction:* The tremendous interest in thermoelectric cooling in the past few years has engendered considerable literature on the subject. (See "References.") In view of the extensive theoretical treatment already available in many of these publications, the following section of this Appendix will present, in summary, mainly those aspects necessary for an understanding of the operation of the thermoelectric thermal barrier.

The theory of thermoelectric devices (both power generating and cooling) involves three interrelated sets of effects, Seebeck, Peltier and Thomson, acting simultaneously. The combination of these effects obviously involves both heat transfer and emf generation phenomena. In consideration of thermoelectric cooling devices, the main emphasis is naturally on heat transfer phenomena. However, emfs induced as secondary effects are of interest because of their influence on the required input power.

*Causes of Phenomena:* The actual mechanisms producing the observed thermoelectric effects are covered in such books on solid-state theory as "Physics of Semiconductors" by A. F. Ioffe, the late Russian authority on thermoelectricity. In general, these phenomena depend on the facts that (1) heat energy, as well as electrical energy, is transported by elemental charge carriers, and (2) charge carriers and their surroundings will interchange energy when one or the other must obtain or lose energy during the accomplishment of a process (e.g., travel of charge carriers from one material to another or application of heat to a junction of two different materials).

The following paragraph, paraphrased from a more complete explanation in "Thermoelectric Phenomena" by Johnson,[46] is included as an example of the types of "microscopic" processes involved:

If an electron current is made to flow from a metal heat transfer surface into an n-type semiconductor at a Peltier couple junction, only those electrons with enough energy to enter via the conduction band do so. Since only these high energy electrons travel, the energy distribution of the remaining electrons in the metal changes from that existing under thermal equilibrium conditions. As a result, the metal must continually furnish energy to these remaining electrons

by means of thermal vibrations, in an attempt to restore the electrons' energy distribution to normal thermal equilibrium conditions. Consequently, as energy is supplied to the electrons by the vibrating metal lattice, the metal becomes cooled. (The fuller explanation in the Johnson publication also covers hole currents and p-type semiconductors.)

*Peltier Effect:* The kind of process just described produces the Peltier effect, the principle of thermoelectric cooling devices: When a current flows across the junction of two dissimilar conductors A and B (Fig. 9), heat is absorbed or liberated at the junction, depending on the direction of current flow. The gross amount of heat absorbed or liberated by the Peltier effect at the junction is:

$$Q_p = \pi_{AB} I = (\pi_A - \pi_B) I \tag{1}$$

where $Q_p$ (watts) = Rate of heat transfer.

$\pi_{AB}$ (volts) = Peltier coefficient. (This quantity, also called the "Peltier voltage," is a function of the coupled materials A and B and the junction temperature.)

$\pi_A$, $\pi_B$ (volts) = Absolute Peltier coefficient for materials A and B at the particular junction temperature.

I (amp) = Current.

(Note: When "amount of heat" is mentioned in this section, it means "amount per unit time," that is, "rate.")

*Seebeck Effect:* The Seebeck effect is the familiar principle of the thermocouples used for temperature measurement. When a circuit consists of two unlike conductors (Fig. 10) and the two junctions of these conductors are at different temperatures, an electromotive force will be produced. The open-circuit thermoelectric or Seebeck emf will be:

$$E_S = S_{AB} \Delta T = (S_A - S_B)(T_h - T_c) \tag{2}$$

where Es (volts) = Seebeck voltage

$S_{AB}$ (volts/°K) = Seebeck coefficient. (This quantity, sometimes erroneously called "thermoelectric power," is a function of the coupled materials A and B.)

$S_A$, $S_B$ (volts/°K) = Absolute Seebeck coefficients for materials A and B. (These are temperature dependent.)

$\Delta T$ (°K) = Temperature difference between hot and cold junctions.

$T_h$ (°K) = Hot junction temperature

$T_c$ (°K) = Cold junction temperature.

*Relationship between Peltier and Seebeck Coefficients:* The Peltier coefficient is related to the Seebeck coefficient by:

$$\pi_{AB} = S_{AB}T \tag{3}$$

where T (°K) = Absolute temperature of junction involved.

Therefore, the equation for heat absorbed due to the Peltier effect can be written:

$$Q_p = S_{AB}T_c \quad I. \tag{4}$$

This relationship is useful because the Seebeck coefficient is more easily measured than the Peltier coefficient.

The Seebeck effect is often considered the converse of the Peltier effect described previously. Actually, the converse of the latter involves the production of an emf (and, consequently, a current) in a *closed* circuit involving two junctions, when these junctions are kept at different temperatures. (This is a second Peltier effect, although *it* is often called the Seebeck effect.) The current produced is related simply to the emf by Ohm's Law.

A consequence of the second Peltier effect is that the production of hot and cold junctions by a thermoelectric current is accompanied by the buildup of a potential at each junction. The net Peltier voltage is in such a direction as to oppose the current. This net Peltier voltage is equal to $(\pi_A - \pi_B)$ at temperature T′ minus $(\pi_A - \pi_B)$ at temperature T. It is not the same as the Seebeck emf because of the Thomson effect.

*Thomson Effect:* If a current passes through a homogeneous conductor in which a temperature gradient exists, the temperature gradient becomes distorted. To prevent this distortion, heat is absorbed from or transferred to the surroundings and a redistribution of heat takes place along the conductor. At the same time, there exists a Thomson emf along the length of the material (see Fig. 11). (The direction of exchange of heat between the conductor and its surroundings and the direction of the emf both depend on the relative directions of current and temperature gradient and on the material.)

The Thomson heat absorbed or generated in a unit volume of conductor is proportional to the temperature gradient and current. The factor of proportionality is called the Thomson coefficient.

The Thomson heat is given by:

$$Q = \tau \frac{dT}{dX} I \tag{5}$$

where Q (watts) = Thomson heat per unit length of conductor.

$\tau$ (volts/°K) = Thomson coefficient of the material

$\frac{dT}{dX}$ (°K/cm) = Temperature gradient.

The Thomson emf is $E_\tau = \int_T^{T'} \tau dT$, where T and T′ are the temperature levels involved.

*Complete Thermoelectric Circuit:* The net Seebeck emf $E_g$ in a thermoelectric circuit (for either cooling or power generation) is comprised of two parts, one associated with the *junctions* (explained by the Peltier effect) and the other associated with the *conductors* (explained by the Thomson effect). The voltages concerned (hence, relationships of the several thermoelectric effects) are shown in Fig. 12

*Other Heat Effects:* The net heat absorbed from the environment at a Peltier cold junction is different than $Q = (\pi_A - \pi_B)I = ST_cI$ because of the flow of heat produced by other causes. These include two irreversible heating effects, Joule and Fourier, and the Thomson heat mentioned above.

The Joule heating $Q_J$ is produced by the $I^2R$ loss through the electrical resistance of the thermoelements and the associated contacts between joined materials.

The Fourier heat $Q_K$ at the cold junction is the leakage heat conducted thermally from the hot junction in accordance with the equation $Q = kA\frac{dT}{dX}$. (In SMM#2, $Q_K$ includes, in effect, the additional heat contribution of the heat-generating element, since this element has an influence on $T_h$ and $T_c$.)

The Thomson effect may produce heating or cooling at a cold junction, depending on types of materials involved. For the materials used in this study, the literature indicates that there is a cooling effect. The Thomson effect is relatively small under usual operating conditions and is ordinarily disregarded in design calculations appearing in the literature.

All three of these heat flows ($Q_J$, $Q_K$, $Q_\tau$) are governed by thermal conduction processes, and, hence, the thermal distribution along the Peltier elements. There is a complex interaction among these three heat flows and the resultant thermal distribution, leading to complicated equations for each heat term, if analyzed rigorously. However, simplifying assumptions can be made. Thus, it can be shown that, in effect, approximately one-half of the Joule heat produced in an element goes to each junction, and that one-half of the Thomson heat goes to (or is removed from) each junction.

*Net Heat Absorbed:* The net heat absorbed at the cold junction is, therefore,

$$Q_c = Q_p - Q_J - Q_K + Q_\tau \tag{6}$$

$$= (S_P - S_N)T_cI - (\tfrac{1}{2}I^2R + I^2R_j) - K(T_h - T_c) + \tfrac{1}{2}\tau(T_h - T_c)I \tag{7}$$

where R (ohms) = Total thermoelement resistance $= \rho_P\frac{l_P}{A_P} + \rho_N\frac{l_N}{A_N}$

$R_j$ (ohms) = Combined contact resistance of all material junctions at cold side

$K\left(\frac{\text{watts}}{°K}\right)$ = Total thermal conductance $= \frac{k_P}{l_P/A_P} + \frac{k_N}{l_N/A_N}$.

In the equations for R and K,

$\rho$(ohm-cm) = Electrical resistivity

$k\left(\frac{\text{watts}}{\text{cm-°K}}\right)$ = Thermal conductivity

l (cm) = Length

A ($cm^2$) = Cross-sectional area.

(The subscripts P and N indicate type of semiconductor material used for thermoelements.)

If ripple is present in the power supply voltage, additional Joule heating results. Correction factors are given in the literature. (See article by Vought in Reference 6 and References 32 and 34.) Using Sickert's method[32] for cases where symmetrical ripple is present, the two $I^2R$ terms in Eq. (7) must be multiplied by $(1 + \phi^2)$, $\phi$ being the current ripple factor expressed as a decimal. Alfonso and Milnes report that ripple as large as 40% may be tolerated under conditions similar to those pertaining to this investigation.

*Cold Junction Heat Balance:* Equations (6) and (7) refer to conditions within any Peltier couple, including the TETB. For equilibrium conditions in the TETB, the net heat $Q_c$ which must be absorbed at the cold junction in accordance with Eq. (6) must equal the external (to the couple) heat loads on the cold junction:

$$Q_c = Q_{hs} + Q_a$$

where $Q_{hs}$ = contribution (directed toward couple) of heat produced by power dissipated in heat-sensitive element (zero in the case of SMM#1 and SMM#2),

$Q_a$ = Ambient heat load.

These heat loads and other thermodynamic conditions pertaining to the simulated micro-modules are shown in Fig. 13, a greatly simplified thermalelectric analog network representing steady-state conditions. (The "resistors" represent thermal resistances to heat flow of pertinent portions of SMM#2 (e.g., wires, encapsulant) and, for purposes of thermal analysis, would be calculated from a knowledge of material thermal parameters and geometries. The thermal resistances relate the various temperature differences and Q's in the same way that electrical resistances relate voltage drops and current. Although it is not intended to present a quantitative thermal analysis in connection with this report, this figure is included to facilitate understanding of TETB operation.)

As mentioned above, $Q_{hs}$ was zero in the simulated micro-modules, but in an actual micro-module would have some finite value. The steady-state value of $T_{hs}$ depends on the heat produced by the heat-sensitive element (through the heat capacity relationship $Q = mc\,(T' - T)$ and surrounding thermodynamic conditions. (Values of $T_{hg}$, the heat produced by the heat-generating element, and surrounding thermodynamic conditions are similarly related.) Since $Q_{hs}$ was zero and the measuring thermocouple was adjacent to the cold transfer surface, $T_{hs}$ in the reported tests was practically equal to $T_c$. The measured heat-generating zone temperature $T_{hgm}$ is at some value between $T_{hg}$ at the heat-generating resistors and $T_h$ at the Peltier couple hot junction.

*Net Heat Liberated:* The heat liberated at the hot junction by the Peltier effect alone is:

$$Q_p' = (S_P - S_N)T_h I. \tag{9}$$

To this is added the Joule contribution $Q_J$ as before. $Q_K$ is subtracted, this being the heat which leaks back toward the cold junction. $Q_\tau$ is subtracted, as the Thomson effect tends to cool the hot side. The net heat liberated (or gained) at the hot junction is, then,

$$Q_h = Q_p' + Q_J - Q_K - Q_\tau \tag{10}$$

$$= (S_P - S_N)T_h I + (\tfrac{1}{2}I^2R + I^2R_j') - K(T_h - T_c) - \tfrac{1}{2}\tau(T_h - T_c)I \tag{11}$$

where $R_j'$ = Combined contact resistance of material junctions at hot side.

*Hot Junction Heat Balance:*

For equilibrium conditions at the hot junction (see Fig. 13), Eq. (6) must equal the net external heat load (or dissipation).

$$Q_h = Q_a' - Q_{hg} \tag{12}$$

where $Q_a'$ = Heat from Peltier couple dissipated to ambient mainly through Peltier lead wires and encapsulant.

$Q_{hg}$ = Contribution (directed toward couple) from heat produced by heat-generating element.

*Electrical Power:* The electrical power required (in watts) is:

$$P = V_t I = Q_h - Q_c = (S_P - S_N)I(T_h - T_c) - \tau(T_h - T_c)I + I^2(R + R_j + R_j') \tag{13}$$

$$= (S_P - S_N - \tau)(T_h - T_c)I + I^2(R + R_j + R_j')$$

where $V_t$ (volts) = Voltage applied to Peltier couple.

(The first term of Eq. (13) includes a back emf which must be overcome by the power input.)

*Coefficient of Performance:*

In heat engineering, the index of performance of a heat transfer machine is the coefficient of performance (C.O.P.), rather than the efficiency. This coefficient of performance for a cooling device is simply the heat removed in unit time from the cooled object divided by the power consumption needed to remove this heat, or

$$\text{C.O.P.} = \frac{Q_c}{P}. \tag{14}$$

*Other Equations:* Other equations of interest to the designer are derived in the literature, with the Thomson effect usually disregarded. In general, designs are directed at either (1) maximum cooling for given current, for economy of material, or (2) maximum coefficient of performance, for economy of power.

*"Maximum Cooling" Equations:*

*Current for maximum cooling:*

$$I_{max} = \frac{ST_c}{R + 2R_j} \tag{15}$$

(Note: R and $R_j$ are combined resistances, as indicated before. Assume $R_j = R_j'$.)

*Maximum cooling rate:*

$$Q_{max} = \tfrac{1}{2}\frac{S^2T_c^2}{R + 2R_j} - K\Delta T. \tag{16}$$

*Maximum temperature difference possible for couple:* (Occurs with no heat load at cold junction.)

$$\Delta T_{max} = \tfrac{1}{2}\frac{S^2T_c^2}{(R + 2R_j)K}. \tag{17a}$$

If contact resistances are neglected, this equation can be rewritten as:

$$\Delta T_{max} = \tfrac{1}{2}ZT_c^2 \tag{17b}$$

where Z ($^\circ K^{-1}$) is the thermoelectric figure of merit. (See Eq. (22).)

If contact resistance is appreciable, an effective figure of merit can be used equal to $\frac{Z}{1 + 2\frac{R_j}{R}}$. This equation indicates the importance of low contact resistance.[6]

*"Maximum Coefficient of Performance" Equations:*

*Current for Maximum C.O.P.:*

$$I_c = \frac{S(T_h - T_c)}{R(\sqrt{1 + ZT_m} - 1)} \tag{18}$$

where Tm (mean temperature) = $\frac{T_h + T_c}{2}$.

$$\text{C.O.P.}_{max} = \frac{T_c}{T_h - T_c} \cdot \frac{\sqrt{1 + ZT_m} - T_h/T_c}{\sqrt{1 + ZT_m} + 1} . \tag{19}$$

(As Z is increased, C.O.P. increases, approaching the ideal Carnot refrigerator coefficient of performance $T_c/(T_h - T_c)$ as a maximum.)

Equations (17b) and (19) indicate that the performance of a thermoelectric cooling device can be expressed solely in terms of the operating temperatures and Z. The higher Z is, the greater is the maximum temperature difference or C.O.P. that can be obtained.

The thermoelectric figure of merit Z of a *couple* is a combination of the parameters S, $\rho$, and k. (These are not constants, but functions of temperature.)

$$Z = \frac{(S_A - S_B)^2}{(\sqrt{k_A \rho_A} + \sqrt{k_B \rho_B})^2} . \tag{20}$$

Where S, $\rho$, and k are equal for both thermoelements, this can be written:

$$Z = \frac{S^2}{k\rho} \tag{21}$$

$$= \frac{S^2}{KR} . \tag{22}$$

Equation (21) is also used to calculate a figure of merit for thermoelectric *material*.

From Eq. (21), it is obvious that a high S and low $\rho$ and k are required to obtain high Z values, such as are needed for practical thermoelectric cooling devices. The century-long delay in utilization of thermoelectric cooling since discovery of the Peltier effect was due to inability to obtain all of these conditions in ordinary materials to the extent desired because of fundamental incompatibility. (For usual materials, high S and high $\rho$ are found together, as is also the case with low k and high $\rho$.) However, certain types of semiconductors can be produced which provide an optimum combination of these material parameters, as indicated in Fig. 14, which shows how S, conductivity $\sigma = \frac{1}{\rho}$ and k vary with the number of charge carriers n in metals, semiconductors and insulators. For thermoelectric materials, n is of the order of $10^{19}$ to $10^{20}\text{cm}^{-3}$ compared to below $10^{16}\text{cm}^{-3}$ for standard semiconductors, and above $10^{23}\text{cm}^{-3}$ for metals. Most favorable are semiconductors with very high mobilities (since conductivity is proportional to mobility, as well as to n) and a poor lattice (thermal) conductivity.

## DISTRIBUTION LIST

| | Copies |
|---|---|
| Commanding General<br>U. S. Army Electronics Command<br>ATTN: AMSEL-AD<br>Fort Monmouth, New Jersey | 3 |
| Office of the Assistant Secretary of Defense<br>(Research and Engineering)<br>ATTN: Technical Library<br>Room 3E1065, The Pentagon<br>Washington 25, D. C. | 1 |
| Chief of Research and Development<br>Department of the Army<br>Washington 25, D. C. | 2 |
| Chief, United States Army Security Agency<br>ATTN: ACofS, G4 (Technical Library)<br>Arlington Hall Station<br>Arlington 12, Virginia | 1 |
| Commanding Officer<br>U. S. Army Electronics Research and Development Activity<br>ATTN: Technical Library<br>Fort Huachuca, Arizona | 1 |
| Commanding Officer<br>U. S. Army Electronics Research and Development Activity<br>ATTN: SELWS-AJ<br>White Sands, New Mexico | 1 |
| Commanding Officer<br>U. S. Army Electronics Research Unit<br>P. O. Box 205<br>Mountain View, California | 1 |
| Commanding Officer<br>U. S. Army Electronics Materiel Support Agency<br>ATTN: SELMS-ADJ<br>Fort Monmouth, New Jersey | 1 |
| Commanding General<br>U. S. Army Satellite Communications Agency<br>ATTN: Technical Documents Center<br>Fort Monmouth, New Jersey | 1 |
| Director<br>U. S. Army Engineer Research and Development Laboratories<br>ATTN: Technical Documents Center<br>Fort Belvoir, Virginia | 1 |
| Commanding Officer<br>U. S. Army Chemical Warfare Laboratories<br>ATTN: Technical Library, Building 330<br>Army Chemical Center, Maryland | 1 |
| Commanding Officer<br>Harry Diamond Laboratories<br>ATTN: Library, Building 92, Room 211<br>Washington 25, D. C. | 1 |
| Headquarters, United States Air Force<br>ATTN: AFCIN<br>Washington 25, D. C. | 2 |
| Rome Air Development Center<br>ATTN: RAALD<br>Griffiss Air Force Base<br>New York | 1 |
| Headquarters<br>Ground Electronics Engineering Installation Agency<br>ATTN: ROZMEL<br>Griffiss Air Force Base<br>New York | 1 |
| Commanding General<br>U. S. Army Materiel Command<br>ATTN: R&D Directorate<br>Washington 25, D. C. | 2 |

## Distribution List (Cont)

| | Copies |
|---|---|
| Aeronautical Systems Division<br>ATTN: ASAPRL<br>Wright-Patterson Air Force Base<br>Ohio | 1 |
| U. S. Air Force Security Service<br>ATTN: ESD<br>San Antonio, Texas | 1 |
| Headquarters<br>Strategic Air Command<br>ATTN: DOCE<br>Offutt Air Force Base, Nebraska | 1 |
| Headquarters<br>Research & Technology Division<br>ATTN: RTH<br>Bolling Air Force Base<br>Washington 25, D. C. | 1 |
| Air Proving Ground Center<br>ATTN: PGAPI<br>Eglin Air Force Base, Florida | 1 |
| Air Force Cambridge Research Laboratories<br>ATTN: CRXL-R<br>L. G. Hanscom Field<br>Bedford, Massachusetts | 2 |
| Headquarters<br>Electronic Systems Division<br>ATTN: ESAT<br>L. G. Hanscom Field<br>Bedford, Massachusetts | 2 |
| AFSC Scientific/Technical Liaison Office<br>U. S. Naval Air Development Center<br>Johnsville, Pa. | 1 |
| Chief of Naval Research<br>ATTN: Code 427<br>Department of the Navy<br>Washington 25, D. C. | 1 |
| Bureau of Ships Technical Library<br>ATTN: Code 312<br>Main Navy Building, Room 1528<br>Washington 25, D. C. | 1 |
| Chief, Bureau of Ships<br>ATTN: Code 454<br>Department of the Navy<br>Washington 25, D. C. | 1 |
| Chief, Bureau of Ships<br>ATTN: Code 686B<br>Department of the Navy<br>Washington 25, D. C. | 1 |
| Director<br>U. S. Naval Research Laboratory<br>ATTN: Code 2027<br>Washington 25, D. C. | 1 |
| Commanding Officer & Director<br>U. S. Navy Electronics Laboratory<br>ATTN: Library<br>San Diego 52, California | 1 |
| Commander<br>U. S. Naval Ordnance Laboratory<br>White Oak<br>Silver Spring 19, Maryland | 1 |
| Commander<br>Armed Services Technical Information Agency<br>ATTN: TISIA<br>Arlington Hall Station<br>Arlington 12, Virginia | 20 |
| USAELRDL Liaison Officer<br>U. S. Army Tank-Automotive Center<br>Detroit Arsenal<br>Center Line, Michigan | 1 |
| USAELRDL Liaison Officer<br>Naval Research Laboratory<br>ATTN: Code 1071<br>Washington 25, D. C. | 1 |
| USAELRDL Liaison Officer<br>Massachusetts Institute of Technology<br>Building 26, Room 131<br>77 Massachusetts Avenue<br>Cambridge 39, Massachusetts | 1 |

## Distribution List (Cont'd)

| | Copies |
|---|---|
| USAELRDL Liaison Office<br>Aeronautical Systems Division<br>ATTN: ASDL-9<br>Wright-Patterson Air Force Base<br>Ohio | 1 |
| U. S. Army Research Liaison Office<br>Lincoln Laboratory<br>P. O. Box 73<br>Lexington, Massachusetts | 1 |
| USAELRDL Liaison Officer<br>Rome Air Development Center<br>ATTN: RAOL<br>Griffiss Air Force Base<br>New York | 1 |
| Commanding Officer<br>U. S. Army Security Agency Processing Center<br>Deal Area, Bldg. 5001 | 1 |
| File Unit Nr. 1, Rm. 3D-116<br>Hexagon | 1 |
| USAEMSA Liaison Engineer<br>USASCAJ<br>APO 343<br>San Francisco, California | 1 |
| Technical Dir., SELRA/CS<br>Headquarters, USAELRDL | 1 |
| USAELRDA-White Sands<br>Liaison Office<br>SELRA/LNW, USAELRDL | 1 |
| AFSC Scientific/Technical<br>Liaison Office<br>SELRA/LNA, USAELRDL | 1 |
| Corps of Engineers<br>Liaison Office<br>SELRA/LNE, USAELRDL | 1 |
| Marine Corps Liaison Office<br>SELRA/LNR, USAELRDL | 1 |
| USACDC Liaison Office<br>SELRA/LNF, USAELRDL | 2 |
| Chief, Technical<br>Information Division<br>Headquarters, USAELRDL | 6 |
| USAELRDL Technical<br>Document Center<br>SELRA/ADL, Hexagon | 1 |
| USAELRDL Liaison Officer<br>U. S. Army Combat Development Command, CDCLN-EL<br>Fort Belvoir, Virginia | 1 |
| Director, Electronic Components Dept., SELRA/P | 1 |
| Director, Electronic Parts and Materials Division, SELRA/PE | 1 |
| Chief, Modular Assemblies Branch, SELRA/PEP | 40 |

AD _____ Div._____

Army Electronics Research and Development Laboratory, Fort Monmouth, N. J.
DESIGN AND EVALUATION OF THERMOELECTRIC THERMAL BARRIER FOR MICRO-MODULES by Robert D. FitzGerald, Herbert C. Frankel. September 1962, 37 p. incl. illus. tables, 51 refs. (USAEIRDL Technical Report 2308) (DA Task 3A99-15-002-03)
Unclassified report

This report covers internal work on the use of a specific Peltier temperature control device, called a "thermoelectric thermal barrier," to protect heat-sensitive electronic circuit elements from closely associated heat-producing elements in a microelectronic assembly. Test results on a simulated binary divider micro-module indicate the feasibility of the thermo-electric thermal barrier approach.

UNCLASSIFIED

1. Thermoelectricity
2. Thermodynamics
3. Heat Transfer
I. FitzGerald, Robert D. Frankel, Herbert C.
II. Army Electronics Research and Development Laboratory, Fort Monmouth, N. J.
III. DA Task 3A99-15-002-03

UNCLASSIFIED

AD _____ Div._____

Army Electronics Research and Development Laboratory, Fort Monmouth, N. J.
DESIGN AND EVALUATION OF THERMOELECTRIC THERMAL BARRIER FOR MICRO-MODULES by Robert D. FitzGerald, Herbert C. Frankel. September 1962, 37 p. incl. illus. tables, 51 refs. (USAEIRDL Technical Report 2308) (DA Task 3A99-15-002-03)
Unclassified report

This report covers internal work on the use of a specific Peltier temperature control device, called a "thermoelectric thermal barrier," to protect heat-sensitive electronic circuit elements from closely associated heat-producing elements in a microelectronic assembly. Test results on a simulated binary divider micro-module indicate the feasibility of the thermo-electric thermal barrier approach.

UNCLASSIFIED

1. Thermoelectricity
2. Thermodynamics
3. Heat Transfer
I. FitzGerald, Robert D. Frankel, Herbert C.
II. Army Electronics Research and Development Laboratory, Fort Monmouth, N. J.
III. DA Task 3A99-15-002-03

UNCLASSIFIED

AD _____ Div._____

Army Electronics Research and Development Laboratory, Fort Monmouth, N. J.
DESIGN AND EVALUATION OF THERMOELECTRIC THERMAL BARRIER FOR MICRO-MODULES by Robert D. FitzGerald, Herbert C. Frankel. September 1962, 37 p. incl. illus. tables, 51 refs. (USAEIRDL Technical Report 2308) (DA Task 3A99-15-002-03)
Unclassified report

This report covers internal work on the use of a specific Peltier temperature control device, called a "thermoelectric thermal barrier," to protect heat-sensitive electronic circuit elements from closely associated heat-producing elements in a microelectronic assembly. Test results on a simulated binary divider micro-module indicate the feasibility of the thermo-electric thermal barrier approach.

UNCLASSIFIED

1. Thermoelectricity
2. Thermodynamics
3. Heat Transfer
I. FitzGerald, Robert D. Frankel, Herbert C.
II. Army Electronics Research and Development Laboratory, Fort Monmouth, N. J.
III. DA Task 3A99-15-002-03

UNCLASSIFIED

AD _____ Div._____

Army Electronics Research and Development Laboratory, Fort Monmouth, N. J.
DESIGN AND EVALUATION OF THERMOELECTRIC THERMAL BARRIER FOR MICRO-MODULES by Robert D. FitzGerald, Herbert C. Frankel. September 1962, 37 p. incl. illus. tables, 51 refs. (USAEIRDL Technical Report 2308) (DA Task 3A99-15-002-03)
Unclassified report

This report covers internal work on the use of a specific Peltier temperature control device, called a "thermoelectric thermal barrier," to protect heat-sensitive electronic circuit elements from closely associated heat-producing elements in a microelectronic assembly. Test results on a simulated binary divider micro-module indicate the feasibility of the thermo-electric thermal barrier approach.

UNCLASSIFIED

1. Thermoelectricity
2. Thermodynamics
3. Heat Transfer
I. FitzGerald, Robert D. Frankel, Herbert C.
II. Army Electronics Research and Development Laboratory, Fort Monmouth, N. J.
III. DA Task 3A99-15-002-03

UNCLASSIFIED